

Implicit regularization via soft ascent-descent

Matthew J. Holland*
Osaka University

Kosuke Nakatani
Osaka University

Abstract

As models grow larger and more complex, achieving better off-sample generalization with minimal trial-and-error is critical to the reliability and economy of machine learning workflows. As a proxy for the well-studied heuristic of seeking “flat” local minima, gradient regularization is a natural avenue, and first-order approximations such as Flooding and sharpness-aware minimization (SAM) have received significant attention, but their performance depends critically on hyperparameters (flood threshold and neighborhood radius, respectively) that are non-trivial to specify in advance. In order to develop a procedure which is more resilient to misspecified hyperparameters, with the hard-threshold “ascent-descent” switching device used in Flooding as motivation, we propose a softened, pointwise mechanism called SoftAD that downweights points on the borderline, limits the effects of outliers, and retains the ascent-descent effect. We contrast formal stationarity guarantees with those for Flooding, and empirically demonstrate how SoftAD can realize classification accuracy competitive with SAM and Flooding while maintaining a much smaller loss generalization gap and model norm. Our empirical tests range from simple binary classification on the plane to image classification using neural networks with millions of parameters; the key trends are observed across all datasets and models studied, and suggest a potential new approach to implicit regularization.

Contents

1	Introduction	2
2	Background (formulation and related work)	3
2.1	Setup	3
2.2	Gradient regularization via linear approximation	4
2.3	Flooding algorithm	5
3	Technique of interest: softened ascent-descent	6
3.1	A concrete implementation	6
3.2	Comparison of latent objective functions	7
3.3	Initial comparison with Flooding mechanism	7
4	Convergence properties	9
4.1	Smooth loss setting	9
4.2	Non-smooth loss setting	11
5	Empirical analysis	12
5.1	Non-linear binary classification on the plane	13
5.2	Image classification from scratch	15

*Corresponding author.

6	Concluding remarks	16
A	Bibliographic notes	18
A.1	Broad overview	18
A.2	Notions of model complexity	18
A.3	Algorithms that generalize well	19
B	Technical appendix	20
B.1	Additional proofs	20
B.2	Gradient of GR objective	22
B.3	Smoothness check	23
C	Empirical appendix	24
C.1	Linear binary classification	24
C.2	Supplement to synthetic data tests in §5.1	26

1 Introduction

Modern machine learning makes use of sophisticated models that are trained through optimization of non-convex objective functions, which typically admit numerous local minima that make for natural candidates when taken at face value.¹ While many such candidates are indeed essentially “optimal” from the viewpoint of classification error rates or other average losses incurred at training time, these often turn out to be highly sub-optimal in terms of *performance at test time*. It goes without saying that understanding and closing this gap is the problem of “generalization” that underlies most machine learning research.²

When we are faced with multiple candidates which are essentially optimal and thus essentially indistinguishable in terms of some “base” objective function (e.g., the average loss) at training time, one of best-known heuristics for identifying good candidates is that of the “landscape” or “geometry” of the base objective in a neighborhood around each candidate. Roughly speaking, one expects that candidates in regions which are in some sense “flat” (often said to be less “sharp”) tend to perform better at test time. Strictly speaking, flatness is not necessary for generalization (Dinh et al., 2017), but our intuition can often be empirically verified to be correct, as good generalization is regularly observed in flat regions where the eigenvalues of the Hessian are mostly concentrated near zero (Chaudhari et al., 2017). The spectral density of the Hessian can in principle be used to evaluate sharpness, and has well-known links to norms that can be used for explicit regularization (Karakida et al., 2019), but for large-scale neural network training in practice, first-order approximations have shown the greatest utility. In particular, the sharpness-aware minimization (SAM) algorithm of Foret et al. (2021), extended for scale invariance by Kwon et al. (2021) and later captured as a special case of the gradient norm penalization (GNP) scheme of Zhao et al. (2022), has shown state-of-the-art performance on a variety of deep learning tasks. As discussed by Karakida et al. (2023), all of these first-order procedures can be cast as (forward) finite-difference approximations of the curvature, requiring *at least* double the computational cost of vanilla gradient descent (GD) at each iteration.

In this work, we study a new method for seeking out local minima that generalize well, without incurring any computational overhead beyond that of vanilla GD. Our approach is

¹We use the term *candidate* to refer to any element of the hypothesis class used for training.

²Large-scale empirical studies are underway; see Jiang et al. (2020) and Dziugaite et al. (2020) to start.

rooted in a risk function design that works as a wrapper for any loss, penalizing both over-performing and under-performing examples to bring about an “ascent-descent” effect similar to the “Flooding” technique studied by Ishida et al. (2020), except that we do not sacrifice smoothness, and we work in a per-point fashion, instead of applying a hard threshold to the whole batch. Our main contributions are as follows:

- We introduce a technique called “softened ascent-descent” (SoftAD), which applies a soft direction-switching mechanism to individual gradients based on their respective loss values, which can then be summed over in batches of arbitrary size. Borderline points are downweighted, and the impact of outlier loss values is bounded; see Figure 4 for an illustration.
- We provide a detailed comparison of SoftAD and its natural alternative, namely the “hard” switching rule encoded in the Flooding algorithm of Ishida et al. (2020). We highlight the smoothness of SoftAD with implications in terms of formal stationarity guarantees, and emphasize how our mechanism leads to update directions that are qualitatively distinct from those used in Flooding.
- Through rigorous empirical tests using both simulated and real-world benchmark classification datasets, featuring neural networks both large and small, we discover that compared with ERM, SAM, and Flooding, the proposed SoftAD achieves far and away the smallest generalization error in terms of the base loss, while maintaining competitive accuracy and small model norms, without any explicit regularization.

Before diving into the main results just described, we introduce notation and background concepts in §2. SoftAD is introduced in §3, and initial empirical comparisons to Flooding are made. In §4 we provide formal guarantees of stationarity for SoftAD and Flooding. Our main empirical test results are given in §5, with discussion and concluding remarks wrapping up the paper in §6. All detailed proofs and supplementary empirical results are relegated to the appendix.

2 Background (formulation and related work)

2.1 Setup

To begin, we formulate the learning problem of interest. For concreteness, let $\mathcal{W} \subseteq \mathbb{R}^d$ be our hypothesis class, let \mathcal{Z} denote the set to which individual data points z belong, and let $\ell : \mathbb{R}^d \times \mathcal{Z} \rightarrow \mathbb{R}$ denote a generic loss function. As is traditional, for the ultimate objective function to be minimized, we select the expected loss, or risk, denoted by $R_\mu(w) := \mathbf{E}_\mu \ell(w; \mathbf{Z})$, where \mathbf{Z} represents a random (test) data point with distribution μ over \mathcal{Z} . While μ is unknown and \mathbf{Z} is not yet observed at training time, we assume the learning algorithm has access to an independent sample of n observations from μ , denoted by $\mathbf{Z}_n := (\mathbf{Z}_1, \dots, \mathbf{Z}_n)$ for convenience. Traditional machine learning algorithms are driven by the empirical risk, denoted here by $R_n(w) := (1/n) \sum_{i=1}^n \ell(w; \mathbf{Z}_i)$, in that they seek out (local) minima of R_n . In this paper, we use the term *empirical risk minimization (ERM)* to refer to algorithms that directly apply an optimizer to R_n . Writing $\mathbf{W}_n := \mathcal{A}(\mathbf{Z}_n)$ for the output of learning algorithm \mathcal{A} (not necessarily ERM), ideally, one would like to design \mathcal{A} such that

$$R_\mu(\mathbf{W}_n) \leq \inf_{w \in \mathcal{W}} R_\mu(w) + \varepsilon \quad (1)$$

holds with sufficiently high probability, where $\varepsilon \geq 0$ represents our tolerance level. For non-linear models such as neural networks, typically the mapping $w \mapsto \ell(w; z)$ is non-convex and

often non-smooth over \mathcal{W} , and thus the usual ERM objective $R_n(\cdot)$ tends to admit a complex landscape.³ This makes it difficult to provide formal guarantees of (global) ε -optimality in the sense of (1), and leads to local minima that can vary significantly in terms of test performance, i.e., a potentially large *generalization gap* $R_\mu(W_n) - R_n(W_n)$. In this paper, our primary practical goal is to achieve a small generalization gap in terms of a pre-specified loss (e.g., cross entropy loss for classification). On top of this, ideally, we would like to achieve this without paying a large price in terms of other metrics (e.g., 0-1 loss, model complexity, algorithm stability, variance over trials, etc.).

2.2 Gradient regularization via linear approximation

Assuming for now that the loss is differentiable, it has been appreciated for some time that the *distribution* of the loss gradients $\nabla \ell(w; Z)$ can convey important information about generalization (Zhang et al., 2020), and in particular the role of gradient regularization, both implicit and explicit, is receiving significant attention (Barrett and Dherin, 2020; Smith et al., 2021).⁴ As a concrete example of explicit regularization, consider modifying the ERM objective using the squared Euclidean norm as

$$\tilde{R}_n(w; \lambda) := R_n(w) + \frac{\lambda}{2} \|\nabla R_n(w)\|^2 \quad (2)$$

where $\lambda \geq 0$ controls the degree of penalization. If one is to minimize this objective in w directly using gradient descent, this involves computing

$$\nabla \tilde{R}_n(w; \lambda) = \nabla R_n(w) + \lambda \nabla^2 R_n(w) (\nabla R_n(w))$$

and thus doing matrix multiplication using a $d \times d$ Hessian $\nabla^2 R_n(w)$, an unattractive proposition when d is large. A linear approximation to the expensive term can be obtained via

$$\frac{\nabla R_n(w + au) - \nabla R_n(w)}{a} \approx \nabla^2 R_n(w) (u)$$

where $u \in \mathbb{R}^d$ is arbitrary and $|a|$ is small.⁵ Applying this to approximate $\nabla \tilde{R}_n(w; \lambda)$, we have

$$\nabla R_n(w) + \frac{\lambda}{a} (\nabla R_n(w + a \nabla R_n(w)) - \nabla R_n(w)) \approx \nabla \tilde{R}_n(w; \lambda). \quad (3)$$

The iterative update directions used by the *SAM* algorithm of Foret et al. (2021) are captured by setting $a = \lambda$, offering a nice link between loss-based sharpness control and gradient regularization. The extension of SAM in GNP (Zhao et al., 2022) can be expressed by an analogous derivation, replacing the squared norm $\|\cdot\|^2$ in (2) with $\|\cdot\|$. Using updates of the form given in (3) with $a > 0$ is called a “forward” finite-difference (FD) approach to explicit gradient regularization (GR) (Karakida et al., 2023) (henceforth, *FD-GR*), and clearly requires two gradient calls per update.⁶ Better precision is available using “centered” FD, at the cost of additional gradient calls.

³See Li et al. (2018) for techniques to visualize the objective function landscape under complex models.

⁴Throughout this paper, all gradients are taken with respect to $w \mapsto \ell(w; z)$, assumed to exist on an open set containing \mathcal{W} for all $z \in \mathcal{Z}$. It should however be noted that gradients taken with respect to parts of the data z have been used in objective function design for years; see Drucker and Le Cun (1992).

⁵See Zhao et al. (2022, §3.3) for example.

⁶In the current example, one call at w , and another call at $w + a \nabla R_n(w)$.

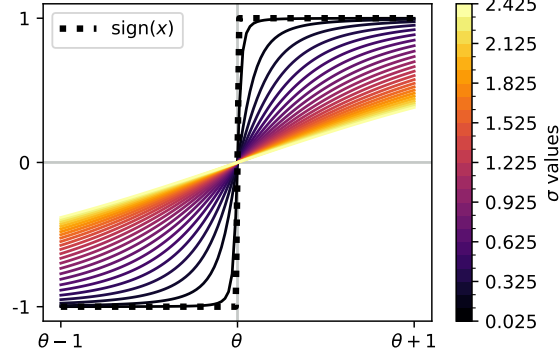


Figure 1: Graphs of the function $x \mapsto \phi_{\text{al}}((x - \theta)/\sigma)$ for different choices of σ , with $\theta = 0$ fixed throughout.

2.3 Flooding algorithm

In order to further reduce the computational cost, one can consider a threshold-based strategy in which the preceding FD-GR update is only applied in certain situations. Consider a sequence (w_1, w_2, \dots) generated using the update

$$w_{t+1} = w_t - \alpha \text{sign}(R_n(w_t) - \theta) \nabla R_n(w_t) \quad (4)$$

for all $t \geq 1$, where $\text{sign}(x) := x/|x|$ for all $x \neq 0$ and $\text{sign}(0) := 0$, and $\alpha > 0$ is a fixed step size. The update (4) is the so-called *Flooding* algorithm studied by Ishida et al. (2020), computing gradients at just one point (here, w_t) for each update index step t . This simple algorithm employs an explicit threshold $\theta \in \mathbb{R}$ with a clear role: above this threshold do gradient descent as usual, below this threshold switch to gradient *ascent* to prevent overfitting.

How does all this relate to the FD-GR update? When the empirical risk goes below the threshold θ , the Flooding update attempts to push it back above θ . Consider the case in which this occurs in a single step, i.e., the situation in which at some step t , the pair of sequential iterates (w_t, w_{t+1}) satisfy the following:

$$R_n(w_t) < \theta \text{ and } R_n(w_{t+1}) > \theta. \quad (5)$$

When condition (5) holds, some basic algebra immediately shows us that running two iterations of the Flooding update (4) yields the equality

$$w_{t+2} = w_t - \alpha^2 \left(\frac{\nabla R_n(w_t + \alpha \nabla R_n(w_t)) - \nabla R_n(w_t)}{\alpha} \right), \quad (6)$$

telling us that the result is equivalent to running one iteration of FD descent with step size α^2 on the GR penalty $\|\nabla R_n(\cdot)\|^2$ at w_t , using the forward FD approximation described earlier in §2.2.⁷ In a sense, this complements the strategy employed in (3); instead of tackling the GR objective $\hat{R}_n(w; \lambda)$ in (2) directly, the Flooding algorithm can iterate back and forth between optimizing the empirical risk and the squared gradient norm. The GR effect is thus constrained to regions in \mathcal{W} with θ -small empirical risk, but all updates outside this region enjoy the same per-step computational complexity as vanilla GD.

On the other hand, from the perspective of achieving a small generalization gap (cf. §2.1), the ascent-descent switching rule encoded in (4) is unwieldy. It was originally proposed as a simple heuristic to harness training losses to allow for better test *accuracy*, but setting the

⁷This point was also highlighted in recent work by Karakida et al. (2023, §5.1).

“best” threshold θ using meticulous validation is both expensive and non-trivial in terms of specifying a set of candidates for θ . This is further complicated by the fact that the ascent-descent switch is determined for all points by the sign of $R_n(\cdot) - \theta$, leaving the “all-in or all-out” switching rule vulnerable to outliers, making the choice of θ based on limited validation data even more difficult. In §3 to follow, we propose a new procedure that retains a threshold-based ascent-descent property, but softens the direction switch in an attempt to make the procedure more resilient to both heavy-tailed loss distributions and misspecified thresholds.

3 Technique of interest: softened ascent-descent

With the context of §2 in place, we consider making two qualitative changes to the Flooding update (4), described as follows.

1. **Pointwise thresholds:** Invert the order of applying $R_n(\cdot)$ and $\text{sign}(\cdot)$, i.e., do summation over data points *after* per-loss truncation.
2. **Soft truncation:** Replace the hard threshold $\text{sign}(\cdot)$ with a continuous, bounded, monotonic (increasing) function $\phi(\cdot)$ satisfying $\phi(0) = 0$.

The reason for making the thresholds pointwise is to allow the algorithm to view “ascent” and “descent” from the perspective of individual losses (rather than bundled up in R_n), making it possible to utilize a sum of both ascent and descent update directions.⁸ To make this sum a *weighted* sum, the soft truncation using ϕ plays a key role. Keeping ϕ bounded limits the impact of errant loss values, while the other assumptions allow for both ascent and descent, with “borderline” points near the threshold given *less* weight. Written explicitly, the proposed update is given as

$$w_{t+1} = w_t - \frac{\alpha}{n} \sum_{i=1}^n \phi(\ell(w_t; Z_i) - \theta) \nabla \ell(w_t; Z_i), \quad (7)$$

where once again $\theta \in \mathbb{R}$ is a fixed threshold, and $\alpha > 0$ is a fixed step size. For convenience, we use *softened ascent-descent* (or *SoftAD* for short) to refer to the algorithm implied by the iterative update (7), assuming ϕ is admissible. Note that for each point being summed over, $\ell(w_t; Z_i) > \theta$ implies descent while $\ell(w_t; Z_i) < \theta$ implies ascent, and borderline points with $\ell(w_t; Z_i) \approx \theta$ have a smaller relative impact.

3.1 A concrete implementation

SoftAD as described in the preceding paragraph specifies a class of algorithms. To make both our theoretical and empirical analysis more concrete, let us consider a specific instance of this class, by setting $\phi = \phi_{\text{al}}$, with ϕ_{al} defined for all $x \in \mathbb{R}$ by

$$\phi_{\text{al}}(x) := \frac{x}{\sqrt{x^2 + 1}}. \quad (8)$$

Noting that for any $x \neq 0$, we clearly have $\phi_{\text{al}}(x) = \text{sign}(x)/\sqrt{1 + x^{-2}}$, from which the desired monotonicity and boundedness follow. It also follows that $\phi_{\text{al}}(x) \rightarrow 0$ as $x \rightarrow 0$. This function is continuously differentiable, and noting that $\phi'_{\text{al}}(x) = 1/(x^2 + 1)^{3/2}$ is bounded, it follows that

⁸This cannot be achieved by taking a mini-batch of size 1 when implementing the Flooding method, since the number of gradients summed over always equals the number of losses averaged when checking the ascent/descent condition.

ϕ_{al} is Lipschitz on \mathbb{R} . There are of course countless other well-known functions which satisfy these properties, and there is nothing particularly special about ϕ_{al} as given in (8); it is just a simple algebraic function, whose derivative and antiderivative both also have simple forms. This simplicity and convenience is likely the reason that it frequently appears in the context of robust statistical estimation.⁹ All the aforementioned properties are preserved by shifted and scaled variants such as $x \mapsto \phi_{\text{al}}((x - \theta)/\sigma)$, for fixed $\theta \in \mathbb{R}$ and $\sigma > 0$. See Figure 1 for an example of how such scaling can control the degree to which $\text{sign}(\cdot)$ is softened.

3.2 Comparison of latent objective functions

Underlying the Flooding update (4) is the empirical objective function

$$\tilde{R}_n^{\text{flood}}(w) := \theta + |R_n(w) - \theta|.$$

This objective is easy to interpret: seek out w such that the empirical risk is as close to threshold θ as possible (either above or below). Even when the empirical risk $R_n(\cdot)$ itself is smooth, depending on the value of θ , note that the Flooding objective $\tilde{R}_n^{\text{flood}}(\cdot)$ need not be differentiable everywhere (i.e., any w such that $R_n(w) = \theta$ and thus cannot be smooth.¹⁰ The Flooding update is simply sub-gradient descent applied to $\tilde{R}_n^{\text{flood}}(\cdot)$, though with a fixed step size α , we certainly cannot expect the candidates (w_t) nor the risk values ($R_\mu(w_t)$) induced by (4) to converge to a locally optimal value in the traditional sense. This is by no means a flaw, but rather a design decision made by Ishida et al. (2020), intended to bring about a “random walk” of sorts along the threshold θ , during which one hopes that the iterates tend to escape from sharp regions.

Let us now contrast the Flooding objective with that which underlies our proposed SoftAD update in (7)–(8). Introducing the function ρ_{al} defined by

$$\rho_{\text{al}}(x) := \sqrt{x^2 + 1} - 1, \quad (9)$$

note that taking derivatives we have $\rho'_{\text{al}}(x) = \phi_{\text{al}}(x)$ for all $x \in \mathbb{R}$, and thus (7) can be seen as gradient descent applied to the following empirical objective:

$$\tilde{R}_n^{\text{AD}}(w) := \theta + \frac{1}{n} \sum_{i=1}^n \rho_{\text{al}}(\ell(w; Z_i) - \theta).$$

The optimal choice of w is thus one in which the average deviations of the incurred losses about θ (as measured by ρ_{al}) are minimized. At first glance, the map $(w, \theta) \mapsto \tilde{R}_n^{\text{AD}}(w)$ looks quite similar to the objectives used in optimized certainty equivalent (OCE) risk minimization (Lee et al., 2020) and some varieties of distributionally robust optimization (DRO) (Duchi and Namkoong, 2021), but the critical difference here is that $\rho_{\text{al}}(\cdot)$ is *not* monotonic. Losses which are too large and too small are *both* penalized. It is precisely this bi-directional property that allows for switching between ascent and descent; this is impossible to achieve with monotonic OCE and DRO risks.¹¹

3.3 Initial comparison with Flooding mechanism

To develop some intuition regarding the differences between our SoftAD procedure (7) and the original Flooding update (4), we carry out a few illustrative numerical experiments. To

⁹A typical smooth Huber function, also known as pseudo-Huber, Charbonnier, and L1-L2 (Barron, 2019).

¹⁰Here “smoothness” is in the sense of having Lipschitz continuous gradients.

¹¹For more background, see recent surveys by Hu et al. (2022); Holland and Tanabe (2022); Royset (2022).

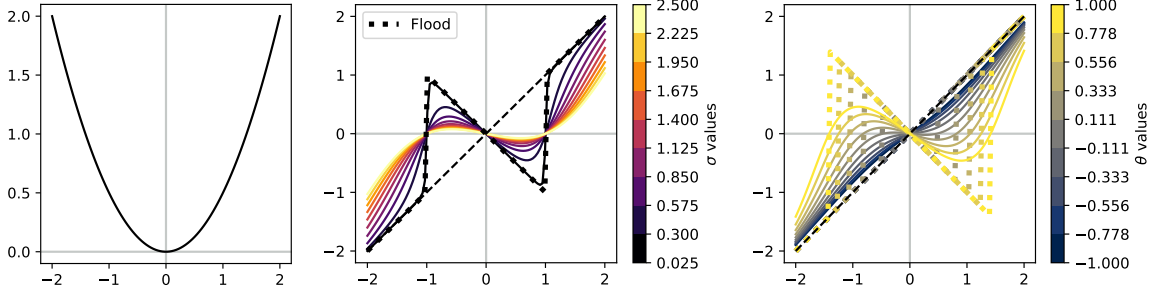


Figure 2: The left-most figure simply plots the graph of $f(x) = x^2/2$ over $x \in [-2, 2]$. The two remaining figures show plots of the graphs of $f'(x) = x$ (dashed black line) and $\phi((f(x) - \theta)/\sigma)f'(x)$ for the same range of x values, with colors corresponding to modified values of σ (middle plot; $\theta = 0.5$ fixed) and θ (right-most plot; $\sigma = 1.0$ fixed) respectively. Thick dotted lines are $\phi = \text{sign}$, thin solid lines are $\phi = \phi_{\text{al}}$.

start, let us consider a simple, non-stochastic example in one dimension. Letting $f : \mathbb{R} \rightarrow \mathbb{R}$ be some differentiable function, we consider how the transformed gradient $\phi(f(x) - \theta)f'(x)$ behaves under $\phi = \text{sign}$ and $\phi = \phi_{\text{al}}$. In Figure 2, we give a numerical example using a quadratic function. The softened nature of the transformed gradients used in SoftAD is clear when compared with the hard switching mechanism underlying the Flooding update.

As we have just seen visually, the soft threshold of SoftAD makes it possible to have Lipschitz gradients, which impacts iterative optimization procedures. For arbitrary values x_1 and x_2 , taking the difference of transformed gradients using arbitrary ϕ , we can write

$$\begin{aligned} & \phi(f(x_1) - \theta)f'(x_1) - \phi(f(x_2) - \theta)f'(x_2) \\ &= (\phi(f(x_1) - \theta) - \phi(f(x_2) - \theta))f'(x_1) + \phi(f(x_2) - \theta)(f'(x_1) - f'(x_2)). \end{aligned} \quad (10)$$

Note that even if $|x_1 - x_2| < \varepsilon$ for some arbitrarily small $\varepsilon > 0$, if for example the threshold is such that $f(x_1) < \theta < f(x_2)$, then under $\phi = \text{sign}$, the difference multiplying $f'(x_1)$ cannot be arbitrarily small, even if f is Lipschitz. On the other hand, such a property follows easily when $\phi = \phi_{\text{al}}$, since ϕ_{al} itself is 1-Lipschitz. In Figure 3, we continue the quadratic function example, looking at sequences (x_1, x_2, \dots) generated based on the Flooding and SoftAD procedures. That is, instead of n points from which to compute losses, we have just one “loss,” namely $f(x) = x^2/2$. Both procedures realize an effective “flood level” of sorts (i.e., a buffer around the loss minimizer), but as expected, the Flooding procedure tends to be far more “jagged” in its trajectory.

Finally, a simple example to illustrate how the per-point soft thresholding of SoftAD leads to distinct gradient-based update directions when compared to the Flooding strategy. Here we consider a dataset of n data points $z_1, \dots, z_n \in \mathbb{R}^2$, and use the squared Euclidean norm as a loss, i.e., $\ell(w; z) = \|w - z\|^2$. This is a natural extension of the quadratic example in the previous paragraph, to multiple points and two dimensions. In Figure 4, we look at two candidate points, and compute the Flooding and SoftAD update directions that arise at each candidate under a randomly generated dataset. We can clearly see how the Flooding update plunges directly towards the minimizer of R_n , unless it is too close (given threshold θ), in which case it goes in the opposite direction. In contrast, the SoftAD update is composed of per-point update directions, some which attract toward the minimum, and some which repel from the minimum, with borderline points down-weighted (shorter update arrows). Since the final update averages over these, movement both toward and away from the minimum is clearly “softened” when compared with the Flooding updates.

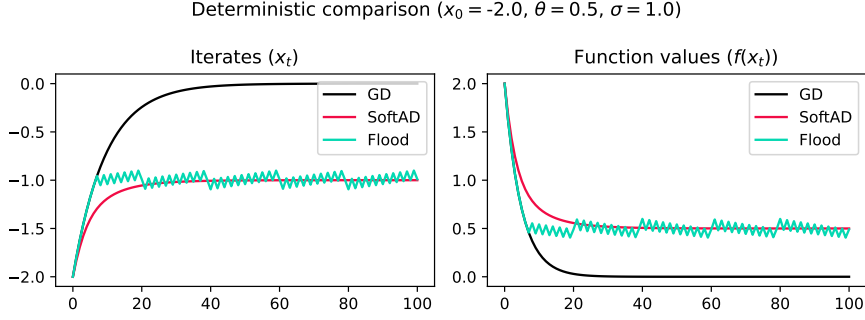


Figure 3: Gradient descent on the quadratic example from Figure 2. The horizontal axis denotes iteration number, and we plot sequences of iterates (x_t) and function values ($f(x_t)$) for each method. Here “GD” denotes vanilla gradient descent, with “Flooding” and “SoftAD” corresponding to (4) and (7)–(8) respectively. Step size is $\alpha = 0.1$.

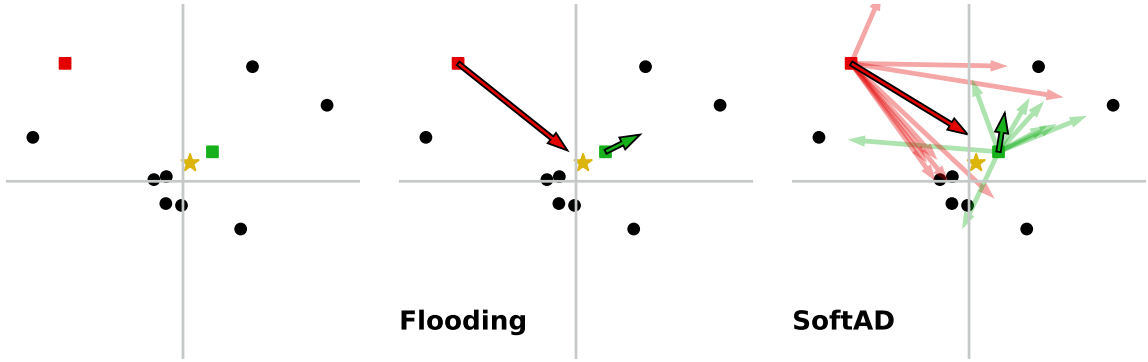


Figure 4: (left) We randomly sample $n = 8$ points (black dots) from the 2D Gaussian distribution, zero mean, zero correlations, with standard deviation $2\sqrt{2}$ in each coordinate. The two candidates are denoted by square-shaped points (red and green), and the minimizer of R_n is given by a gold star. (center) The Flooding updates (colored arrows) via (4) for each candidate. (right) Analogous SoftAD update vectors via (7), with per-point transformed gradients (semi-transparent arrows) for reference. Throughout, we have fixed $\theta = 1.5 \times \min_w R_n(w)$ and $\alpha = 0.75$.

4 Convergence properties

With the Flooding and SoftAD methods in mind, next we consider concrete conditions under which stochastic gradient-based learning algorithms can be given guarantees of (approximate) stationarity. Throughout this section, we assume that the loss $w \mapsto \ell(w; z)$ is locally Lipschitz on \mathcal{W} for each $z \in \mathcal{Z}$, but convexity will not be used, and differentiability will only be assumed in §4.1. In addition, let us assume for simplicity that (Z_1, Z_2, \dots) is a sequence of independent random variables with distribution μ , the same as our test data point $Z \sim \mu$.

4.1 Smooth loss setting

When the losses are sufficiently smooth, it is straightforward to implement SoftAD in such a way that lucid stationarity guarantees are possible. More precisely, assuming the underlying loss is differentiable, and letting $\phi : \mathbb{R} \rightarrow \mathbb{R}$ be an arbitrary function for the time being, we are interested in learning algorithms fuelled by gradient vectors of the form

$$G_t(w) := \phi(\ell(w; Z_t) - \theta) \nabla \ell(w; Z_t) \quad (11)$$

for all integers $t \geq 1$ and $w \in \mathcal{W}$, with threshold $\theta \in \mathbb{R}$ fixed in advance.

SoftAD algorithm Recalling §3.2, the underlying *population* objective is

$$\tilde{R}_\mu^{\text{AD}}(w) := \theta + \mathbf{E}_\mu \rho_{\text{al}}(\ell(w; \mathbf{Z}) - \theta). \quad (12)$$

By design, we cannot expect SoftAD to approach a stationary point of the original R_μ . On the other hand, note that by setting $\phi = \phi_{\text{al}}$ in (11) (a mini-batch variant of (7)), we have unbiased estimators of gradients of the modified objective (12). As such, stationarity in terms of this target is a reasonable goal. Assuming the losses are L_ℓ -smooth in expectation, using the equality (10) one can readily confirm that the objective (12) is L_{AD} -smooth, with

$$L_{\text{AD}} := \mathbf{E}_\mu \left[\sup_{w \in \mathcal{W}} \|\nabla \ell(w; \mathbf{Z})\|^2 \right] + L_\ell. \quad (13)$$

A more detailed derivation is given in §B.3. Assuming that second-order moments are finite in a uniform sense over \mathcal{W} ensures that $L_{\text{AD}} < \infty$, and naturally implies pointwise variance bounds, allowing us to seek out stationarity guarantees using a combination of gradient norm control and momentum in the fashion of Cutkosky and Mehta (2021).

Proposition 1 (Stationarity for SoftAD, smooth case). *Starting with an arbitrary $w_1 \in \mathcal{W}$, update using $w_{t+1} = w_t - \alpha \mathbf{M}_t / \|\mathbf{M}_t\|$, where $\mathbf{M}_t := b\mathbf{M}_{t-1} + (1-b)\bar{\mathbf{G}}_t(w_t)$ for $t \geq 1$, with $\mathbf{M}_0 := 0$ and $\bar{\mathbf{G}}_t(\cdot) := \mathbf{G}_t(\cdot) \min\{1, \gamma / \|\mathbf{G}_t(\cdot)\|\}$, taking each gradient $\mathbf{G}_t(\cdot)$ based on (11) with $\phi = \phi_{\text{al}}$ as in §3.1. Assuming we make $T-1$ updates, set the momentum parameter to $b = 1 - 1/\sqrt{T}$, the norm threshold to $\gamma = \sqrt{(L_{\text{AD}} - L_\ell)/(1-b)}$, and the step size to $\alpha = 1/T^{3/4}$. The stationarity of this sequence (w_1, w_2, \dots) , assumed to be in \mathcal{W} , in terms of the modified objective (12) can be bounded by*

$$\frac{1}{T} \sum_{t=1}^T \|\nabla \tilde{R}_\mu^{\text{AD}}(w_t)\| \leq \frac{1}{T^{1/4}} \left(\tilde{R}_\mu^{\text{AD}}(w_1) - \tilde{R}_\mu^{\text{AD}}(w_{T+1}) + \frac{3L_{\text{AD}}}{2} + 2\sqrt{L_{\text{AD}} - L_\ell} (1 + C_\delta) \right)$$

using confidence-dependent factor

$$C_\delta := 10 \log(3T/\delta) + 4\sqrt{\log(3T/\delta)} + 1, \quad (14)$$

with probability no less than $1 - \delta$ over the draw of $(\mathbf{Z}_1, \mathbf{Z}_2, \dots)$.

Flooding algorithm For comparison, we next consider stationarity of the Flooding algorithm in the same context of smooth losses. The argument used in Proposition 1 critically depends on the smoothness of the underlying objective (12). As discussed in §3.2, this smoothness cannot be leveraged when we consider the natural analogue for Flooding, namely the function

$$w \mapsto \theta + |R_\mu(w) - \theta|. \quad (15)$$

Further complicating things is the fact that stochastic gradients of the form (11) do not yield unbiased sub-gradient estimates for (15), but rather for an upper bound $\theta + \mathbf{E}_\mu |\ell(w; \mathbf{Z}) - \theta|$ that follows via Jensen’s inequality. A lack of smoothness means we cannot establish stationarity in terms of (15) nor the upper bound just given, but it is possible using a smoothed approximation (the Moreau envelope) of this bound:

$$\tilde{R}_\mu^{\text{flood}}(w) := \inf_{v \in \mathcal{W}} \left[\theta + \mathbf{E}_\mu |\ell(v; \mathbf{Z}) - \theta| + \frac{1}{2\beta} \|v - w\|^2 \right]. \quad (16)$$

The parameter $\beta > 0$ controls the degree of smoothness. The objective in (16) can be linked to “gradients” in (11) with $\phi = \text{sign}$, and leveraging the Lipschitz continuity of $|\cdot|$ along with a

sufficiently smooth loss, it is possible to show that this non-smooth objective satisfies a weak form of convexity, and using the techniques of [Davis and Drusvyatskiy \(2019\)](#) it is possible to show that stochastic gradient algorithms enjoy stationarity guarantees, albeit not in terms of the objective (15), but rather the smoothed upper bound (16).

Proposition 2 (Stationarity for Flooding, smooth case). *Letting \mathcal{W} be closed and convex, take an initial point $w_1 \in \mathcal{W}$, and make $T - 1$ updates using $w_{t+1} = \Pi_{\mathcal{W}}[w_t - \alpha \mathbf{G}_t(w_t)]$, where $\Pi_{\mathcal{W}}[\cdot]$ denotes projection to \mathcal{W} , and each $\mathbf{G}_t(\cdot)$ is computed using (11) with $\phi = \text{sign}$. Assuming the loss $w \mapsto \ell(w; z)$ is L_ℓ^* -smooth on \mathcal{W} for all $z \in \mathcal{Z}$, and taking a step size of*

$$\alpha^2 = \frac{\Delta}{TL_\ell^*(L_{\text{AD}} - L_\ell)}, \text{ using } \Delta \text{ such that } \Delta \geq \tilde{\mathbf{R}}_\mu^{\text{flood}}(w_1) - \inf_{w \in \mathcal{W}} \tilde{\mathbf{R}}_\mu^{\text{flood}}(w),$$

with L_{AD} and L_ℓ as in (13), the expected squared stationarity in terms of the smoothed upper bound (16) at smoothness level $\beta = 1/(2L_\ell^*)$ can be controlled as

$$\frac{1}{T} \sum_{t=1}^T \mathbf{E} \|\nabla \tilde{\mathbf{R}}_\mu^{\text{flood}}(w_t)\|^2 \leq \sqrt{\frac{2L_\ell^*(L_{\text{AD}} - L_\ell)\Delta}{T}}$$

with expectation taken over the draw of $(\mathbf{Z}_1, \mathbf{Z}_2, \dots)$.

Remark 3 (Comparing rates and assumptions). Considering the preceding Propositions 1 and 2, one common point is that learning algorithms based on both the SoftAD and Flooding gradients (of mini-batch size 1) can be shown to be approximately stationary in terms of functions of a similar form (i.e., (12) and (15)), differing only in how they measure deviations from the threshold θ . The rates of decrease (as a function of T) are essentially the same, noting that the bounds in Proposition 2 are in terms of *squared* norms. That said, a lack of smoothness means the Flooding guarantees only hold for a smoothed variant, plus they require a stronger form of smoothness in the loss (over all z vs. in expectation). In addition, the SoftAD guarantees hold with high probability over the data sample, and can be readily strengthened to hold for an individual iterate (instead of summing over T iterates), using for example the technique of [Cutkosky and Mehta \(2021, Thm. 3\)](#).

4.2 Non-smooth loss setting

All of the analysis in the previous sub-section relied heavily on smoothness of the underlying loss function. Here we consider the case in which the loss itself may not even be differentiable. All we ask is that the losses be L -Lipschitz on \mathcal{W} in expectation, i.e., $\mathbf{E}_\mu |\ell(w_1; \mathbf{Z}) - \ell(w_2; \mathbf{Z})| \leq L\|w_1 - w_2\|$ for all $w_1, w_2 \in \mathcal{W}$. To formulate an explicit objective function, let us write

$$\tilde{\mathbf{R}}_\mu(w) := \theta + \mathbf{E}_\mu \rho(\ell(w; \mathbf{Z}) - \theta) \tag{17}$$

with $\theta \in \mathbb{R}$ as a fixed threshold as usual, and $\rho : \mathbb{R} \rightarrow \mathbb{R}_+$ a generic 1-Lipschitz function, capturing the two special cases of interest, $\rho = \rho_{\text{al}}$ (for SoftAD) and $\rho(\cdot) = |\cdot|$ (for Flooding). Shifting our focus to function values (rather than gradients), we will also need to assume a second moment bound

$$\mathbf{E}_\mu (\theta + \rho(\ell(w; \mathbf{Z}) - \theta))^2 \leq V < \infty \tag{18}$$

that holds over $w \in \mathcal{W}$. With these basic assumptions in place, stationarity guarantees are available via a smooth approximation.

Proposition 4 (Stationarity, non-smooth case). *Choosing an initial value $w_1 \in \mathcal{W}$, run the algorithm described in Proposition 1, re-defining the core gradients based on (17) as*

$$\mathbf{G}_t(w) := \frac{d}{r} (\theta + \rho(\ell(w + r\mathbf{U}_t; \mathbf{Z}_t) - \theta)) \mathbf{U}_t$$

where $(\mathbf{U}_1, \mathbf{U}_2, \dots)$ is a sequence of independent vectors sampled uniformly at random from the unit sphere, and $r > 0$ sets the smoothing radius. In addition, the norm threshold is set as $\gamma = \sqrt{dL}/((1-b)r)$ (with b unchanged). Stationarity of the resulting sequence (w_1, w_2, \dots) , assumed to be in \mathcal{W} , can be controlled with probability $1 - \delta$ as

$$\frac{1}{T} \sum_{t=1}^T \|\nabla \bar{\mathbf{R}}_\mu(w_t; r)\| \leq \frac{1}{T^{1/4}} \left(\bar{\mathbf{R}}_\mu(w_1) - \bar{\mathbf{R}}_\mu(w_{T+1}) + \frac{3dL}{2r} + \frac{2d}{r} \sqrt{V} (1 + C_\delta) \right)$$

where $\bar{\mathbf{R}}_\mu(w; r) := \mathbf{E}[\tilde{\mathbf{R}}_\mu(w + r\mathbf{V})]$ is the r -smoothed approximation of the objective (17), with \mathbf{V} distributed uniformly over the unit ball. Probability is taken over the random draw of $(\mathbf{Z}_1, \mathbf{Z}_2, \dots)$ and $(\mathbf{U}_1, \mathbf{U}_2, \dots)$, and the confidence factor C_δ matches that of (14).

Remark 5 (Stationarity in the original objective). When the original objective $\tilde{\mathbf{R}}_\mu(\cdot)$ given in (17) is sufficiently well-behaved, e.g., differentiable almost everywhere and Lipschitz, then stationarity guarantees in terms of the r -smoothed objective $\bar{\mathbf{R}}_\mu(\cdot; r)$ can be easily translated into analogous guarantees for $\tilde{\mathbf{R}}_\mu(\cdot)$. In addition, very recent work by Cutkosky et al. (2023) shows how a modified algorithmic approach can be used to achieve faster rates under such congenial (but still non-convex and non-smooth) conditions.

5 Empirical analysis

In this section, we apply the proposed SoftAD procedure to a variety of classification tasks using neural network models, leading to losses that are non-convex and non-smooth (e.g., non-linear NNs including ReLU activations). Our goal here is to compare and contrast the behavior of SoftAD with three natural alternatives: ERM, Flooding, and SAM.¹² In §5.1, we essentially recreate the tests using synthetic data run by Ishida et al. (2020, §4.1), which compared Flooding and ERM; we simply add SoftAD and SAM into the mix. In §5.2, we use several well-known benchmark image classification datasets to train neural network models from scratch. We have essentially modeled the experiment design after analogous tests done by Ishida et al. (2020, §4.2) and Foret et al. (2021, §3.1), but since our focus is on a clear comparison on the original data rather than achieving state-of-the-art accuracy, we have not included optional tweaks such as data augmentation and early stopping as seen in these previous works.

Software and hardware All of the experiments done in this section have been implemented using PyTorch 2, utilizing three machines each using a single-GPU implementation, i.e., there is no parallelization across multiple machines or GPUs. Two units are equipped with an NVIDIA A100 (80GB), and the remaining machine uses an NVIDIA RTX 6000 Ada. We use the MLflow library for storing and retrieving metrics and experiment details. To re-create all of the numerical test results and figures from this paper, source code and Jupyter notebooks are available at a public GitHub repository.¹³

¹²Our coding of SAM follows that of David Samuel (<https://github.com/davda54/sam>), which is the PyTorch implementation acknowledged in the original SAM paper of Foret et al. (2021).

¹³<https://github.com/feedbackward/bdd-flood>



Figure 5: Synthetic dataset examples. From left to right: “two Gaussians,” “sinusoid,” and “spiral.”

5.1 Non-linear binary classification on the plane

Our first set of experiments considers a simple binary classification task on the plane, using three synthetic data-generating mechanisms to create a dataset that is not linearly separable, but nearly separable using a simple non-linear model (up to label noise). The models underlying the data are left unknown, and we train a simple feedforward neural network to classify.

Data The three types of synthetic data that we generate here differ chiefly in the degree of non-linearity; see Figure 5 for an example. The “two Gaussians” dataset is almost linearly separable, save for some overlap of the two distributions. The “sinusoid” data is separated by a simple curve, easily approximated by a low-order polynomial, but the curves in the “spiral” data are a bit more complicated. Exact implementation details, plus historical references, are given by Ishida et al. (2020, §4.1). For each trial, we generate training and validation data of size 100, and test data of size 20000. All methods see the same data in each trial. In addition to the original “clean” data, we also consider “noisy” data, where 5% of the binary labels (training, validation, and test sets) are flipped at random.

Model For each dataset, we use the same model, namely a simple feedforward neural network with four hidden layers, 500 units per layer, using batch normalization and ReLU activations at each layer.¹⁴

Algorithms In line with the experiments we are trying to replicate, all methods (ERM, Flooding, SAM, and SoftAD) are driven by the Adam optimizer, using a fixed learning rate of 0.001, with no momentum or weight decay. All methods use the multi-class logistic loss as their base loss (i.e., `nn.CrossEntropyLoss` in PyTorch), and are run for 500 epochs. The original tests in Ishida et al. (2020) used a full batch (of 100); we also consider mini-batch runs here.

Hyperparameter selection ERM has no hyperparameters, but all the other methods have one each. Flooding and SoftAD both have the threshold parameter θ seen in §2–§4, and SAM has a radius parameter (denoted “ ρ ” in the original paper). For each of these methods, in each

¹⁴Ishida et al. (2020) say they use a “five-hidden-layer feedforward neural network,” but looking at their public code, the number of hidden layers (i.e., number of linear transformations excluding that of the output layer) is actually four.

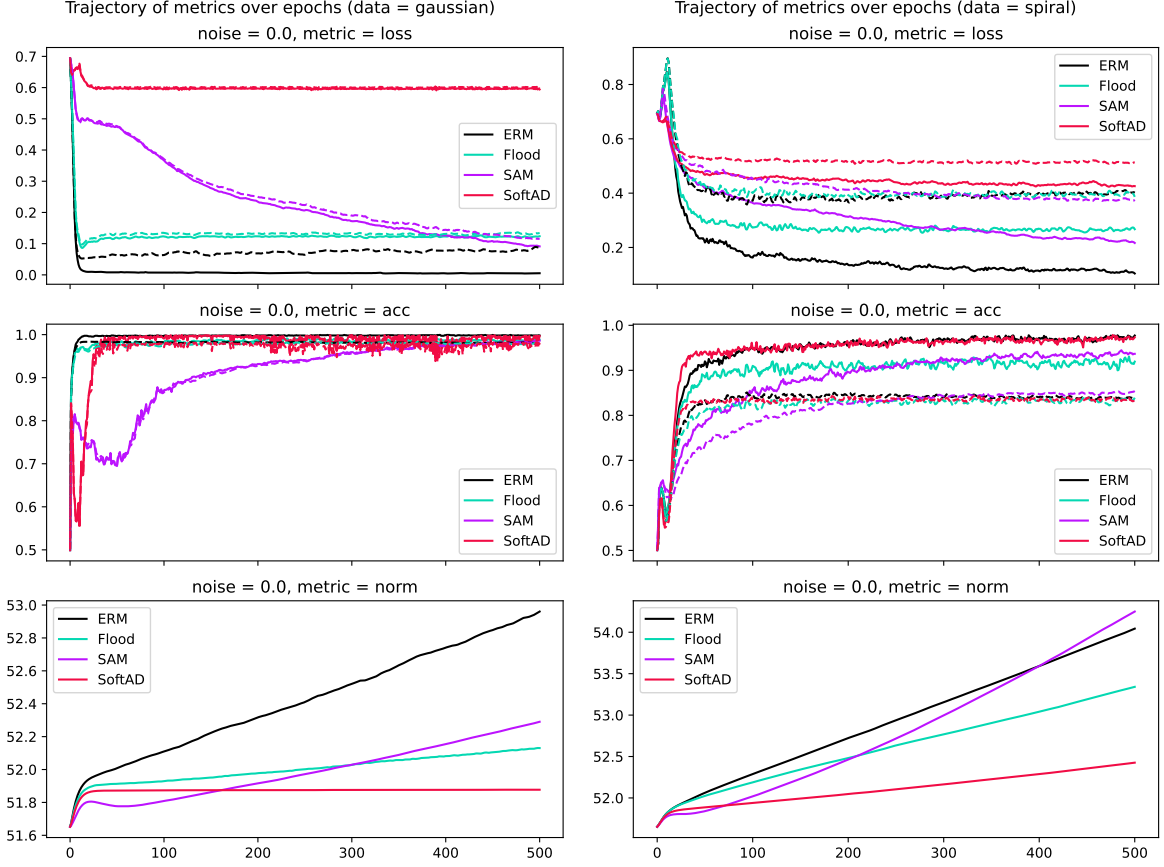


Figure 6: Representative results from synthetic experiments described in §5.1. Training and test metrics are denoted by solid and dashed curves, respectively. Note that SoftAD achieves competitive accuracy at a much higher loss level than other methods, with much smaller norm.

trial, we select from a grid of 40 points spaced linearly between 0.01 and 2.0. Selection is based on classification accuracy on validation data.

Main results In Figure 6 we give representative results for the “two Gaussians” and “spiral” datasets, without label noise, using mini-batch size of 50. We plot three different types of metrics as a function of epoch number: average loss (top), classification accuracy (middle), and the norm of model parameters (bottom). These metrics are recorded at the time of initialization (epoch number 0), and after each training epoch. We have run 15 independent trials, and all metrics shown are averages taken over trials. For the loss and accuracy trajectories, we give metrics in terms of both training data (solid curve) and test data (dashed curve). Perhaps the most salient feature we can read from these figures is the fact that SoftAD can match or exceed the accuracy of the best competitors while incurring a *much* larger loss. SoftAD results in by far the smallest model norm as well as training-testing generalization gap in terms of *losses*. On the other hand, while test accuracy is competitive, the training-testing gap is actually the largest of all methods seen. These trends hold across all the datasets tested, with and without noise, using both full-batch and mini-batch settings.¹⁵

¹⁵Additional figures are provided in the appendix §C.2.

5.2 Image classification from scratch

Our second set of experiments utilizes four well-known benchmark datasets for multi-class image classification. Compared to the synthetic experiments done in §5.1, the classification task is more difficult (much larger inputs, variation within classes, more classes), and so we utilize more sophisticated neural network models to tackle the classification task. That said, as the sub-section title indicates, this training is done “from scratch,” i.e., no pre-trained models are used.

Data The datasets we use are all standard benchmarks in the machine learning community: CIFAR-10, CIFAR-100, FashionMNIST, and SVHN. All of these datasets are collected using classes defined in the `torchvision.datasets` module, with raw training/test splits left as-is with default settings. As such, across all trials the test set is constant, but in each trial we randomly select 80% of the raw training data to be used for actual training, with the remaining 20% used for validation. We normalize all pixel values in the image data to the unit interval $[0, 1]$; this is done separately for training, validation, and testing data.

Models Unlike the previous sub-section, here we use different models for different data sets. Model choice essentially mirrors that of Ishida et al. (2020, §4.2). For FashionMNIST, we flatten each image into a vector, and use a simple feedforward neural network composed of a single hidden layer with 1000 units, batch normalization, and ReLU activation before the output transformation. For SVHN, we use ResNet-18 as implemented in `torchvision.models`, without any pre-trained weights. Finally, for both CIFAR-10 and CIFAR-100, we use ResNet-34 (again in `torchvision.models`) without pre-training. Both of the ResNet models used do not flatten the images, but rather take each RGB image as-is.

Algorithms Just as in §5.1, we are testing ERM, Flooding, SAM, and SoftAD. Again we use the cross entropy loss, and run for 500 epochs. However, instead of Adam as the base optimizer, here we use vanilla SGD with a fixed step size of 0.1, and momentum parameter of 0.9. For all datasets, we use a mini-batch size of 200. All these settings match the experimental setup of Ishida et al. (2020, §4.2).¹⁶

Hyperparameter selection Once again we select hyperparameters for Flooding, SoftAD, and SAM from a grid of candidate values, such that the classification accuracy on validation data is maximized. Unlike §5.1 however, here we use different grids for each method. For Flooding, we follow the setup of the original paper, choosing from ten values: $\{0.01, 0.02, \dots, 0.1\}$. For SAM, once again we follow the original paper (their §3.1), which for analogous tests utilized the set $\{0.01, 0.02, 0.05, 0.1, 0.2, 0.5\}$. Finally, for SoftAD we match the set size used by Flooding (i.e., ten) by taking the union of $\{0.15, 0.25, 0.35, 0.75\}$ and the set used by SAM.

Main results In Figures 7 and 8, once again we provide the trajectories over epochs for average loss, classification accuracy, and model norm, for each of the methods of interest. All metrics are averaged over five independent trials. These plots are analogous to those given in Figure 6 of §5.1. Despite using larger datasets, much more complicated models, and a different base optimizer (SGD instead of Adam), the key trends observed in the synthetic tests hold across the benchmark data tests as well. It is clear that SoftAD works very well as a

¹⁶Batch size is not given in the original Flooding paper, but the size of 200 was confirmed by means of a private communication with the authors.

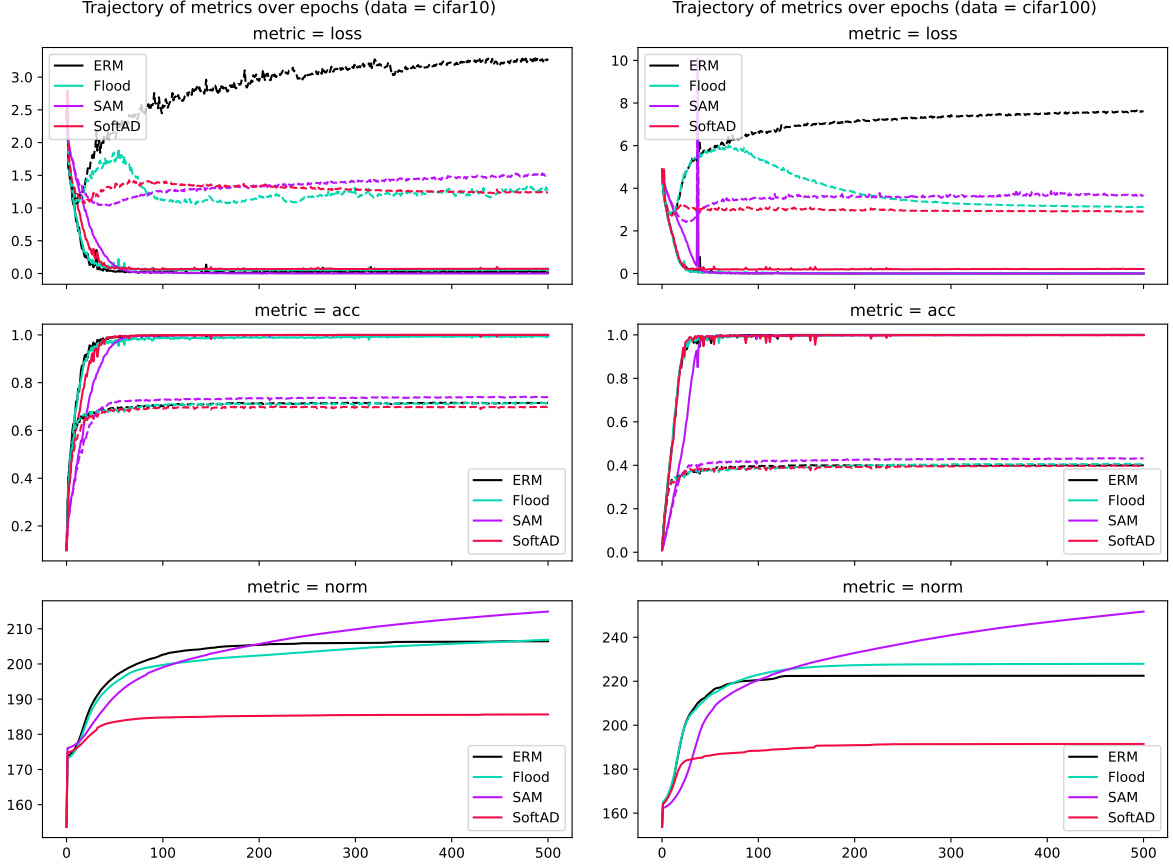


Figure 7: Results from benchmark tests described in §5.2 for CIFAR- $\{10, 100\}$. Training and test metrics are denoted by solid and dashed curves, respectively. As with the synthetic test results in Figure 6, SoftAD is shown to be able to achieve competitive accuracy at a higher (training) loss level than other methods, with the smallest norm and loss generalization gap.

regularizer in terms of the model norm and achieving the smallest generalization gap (in losses) while maintaining high training accuracy. It should be noted that this is achieved using *half* the gradient computations made by SAM. It is also rather remarkable that despite high training accuracy at the smallest model norm with minimum loss error gap, only the training-testing accuracy gap remains comparatively large.

6 Concluding remarks

In this paper, we have introduced SoftAD, a simple modification to existing hard-threshold rules for iterative switching between ascent and descent, which retains smoothness and treats losses/gradients in a pointwise fashion. As stated in §2.1, our primary goal here has been to design a general-purpose learning algorithm that achieves a good tradeoff between the generalization gap in some base loss and other factors such as accuracy, model complexity, and computational cost. To this extent, the empirical results of §5 provide strong initial evidence that the SoftAD procedure achieves a very competitive tradeoff, even when compared with well-studied methods such as Flooding and SAM. It is particularly notable that for all settings considered, SoftAD has the best (smallest) loss generalization gap and model norm, often by a wide margin, paying a small price in test accuracy. Whether “small” means “negligible” or not

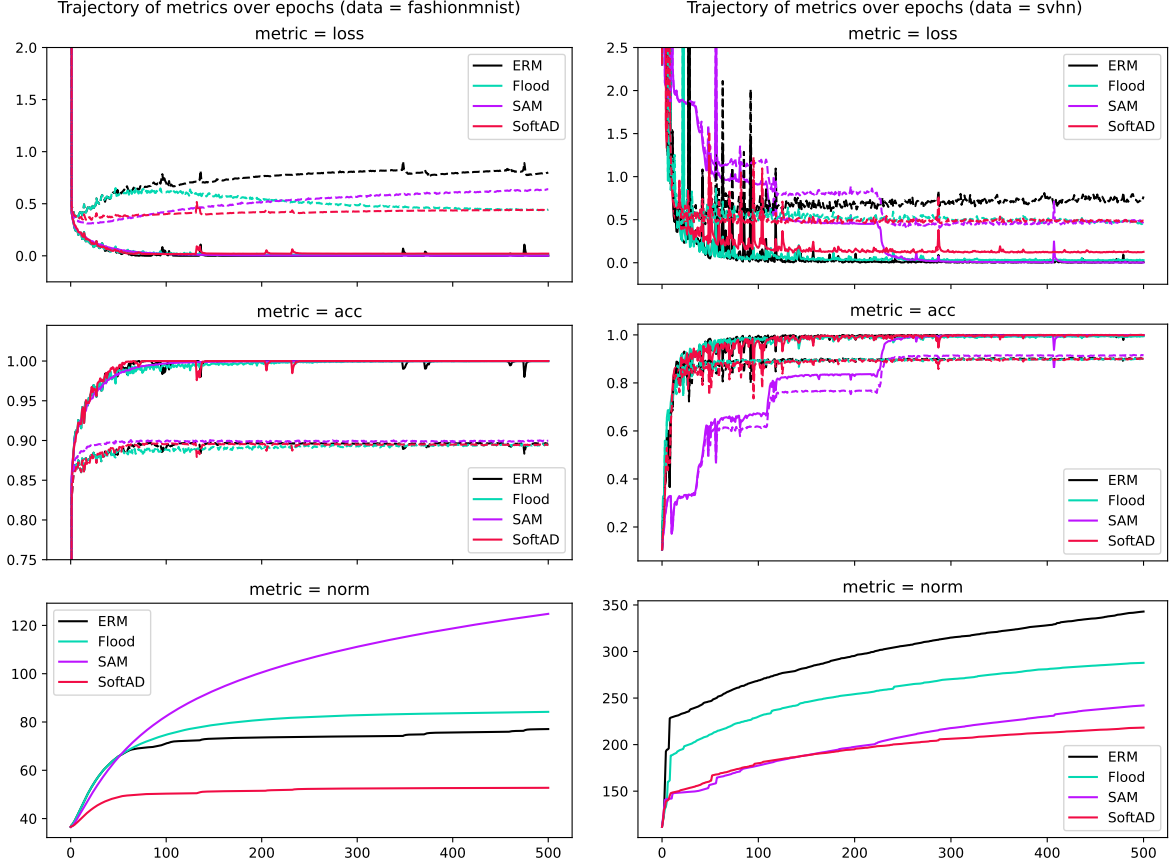


Figure 8: Analogous to Figure 7, for FashionMNIST and SVHN.

is of course arguable, and the degree to which this price can be reduced by further algorithmic modifications is a natural direction for future research. In particular, automated strategies for setting θ in a more cost-effective manner (than naive validation) is of great interest, both in terms of basic theory and practical utility. The generalization gap in *accuracy* seems unusually large given the small gap for losses and high training accuracy; we intend to pursue further studies using a much wider class of loss functions (only cross-entropy and 0-1 were used in §5), and hope to paint a clearer picture in terms of tradeoffs, including considerations of neural network calibration (Guo et al., 2017). Finally, the strong effect of SoftAD on the model norm is of independent interest. Karakida et al. (2023, §4.3) discuss a theoretical link between FD-GR methods and implicit regularization using diagonal linear networks, and we hope to use an analogous framework to shed light on the norm control brought about implicitly by the SoftAD technique studied here.

A Bibliographic notes

In this section, we provide additional references intended to complement those in the main body of the paper.

A.1 Broad overview

The following questions succinctly summarize key aspects of the problem of generalization.¹⁷

QP. What properties at training time are reliable indicators of performance at test time?

QA. How can we efficiently find candidates with such desirable properties?

The easy answer to these questions is, of course, “it depends.” There is no fixed procedure that can guarantee arbitrarily good performance on all statistical learning problems, even if restricted to binary classification tasks.¹⁸ A more subtle answer involves characterizing the problems on which abstract learning algorithms such as empirical risk minimization (ERM) yield tight bounds on tractable criteria of interest (e.g., the expected loss).¹⁹ Even more difficult is refining our understanding of the learning problems on which concrete algorithms used in practice can be reliably expected to perform well.²⁰

For conceptual grounding, we make use of the two questions, QP (the “property” question) and QA (the “algorithm” question), particularly within the context of non-linear models such as neural networks. Broadly speaking, in the machine learning literature over the past three decades, most answers to the property question QP come in the form of quantifying some notion of “simplicity,” a property of candidate w . It goes without saying that the underlying heuristic is that all else equal (at training time), a “complex” candidate seems intuitively less likely to perform well at test time.²¹ As for the algorithm question, there are numerous “workhorse” procedures of machine learning that are computationally convenient, have high-quality software available, and tend to generalize very well in practice, providing a partial answer to QA. That said, the design principles underlying these procedures are often only very loosely related to the properties that satisfy QP.²² With this in mind, a large body of research can be understood as trying to develop new connections between answers to QP and QA, either through *post hoc* analysis using existing concepts, or by introducing new properties and deriving algorithms in a more unified fashion.

A.2 Notions of model complexity

Model complexity is a concept that has a long history in the context of statistical model selection (Claeskens and Hjort, 2008), with well-established ties to information theory (Kullback, 1968). Assuming the quality of “fit” is measured using negative log-likelihood, the second derivative of this objective function (Hessian matrix in multi-dimensional case) is known as the Fisher information (matrix).²³ In the context of neural networks, it is common to use their

¹⁷These questions are inspired by the concise and lucid problem setting of Jia and Su (2020).

¹⁸A lucid explanation is given by Devroye et al. (1996, Ch. 1).

¹⁹Even this refined problem is far from trivial; see Shalev-Shwartz et al. (2010) and Feldman (2016).

²⁰Even the critical question of which core optimizer to use does not have a clear-cut answer on standard benchmark datasets (Schmidt et al., 2021). With additional options such dropout, batch normalization, and all manners of data augmentation, it is not surprising that the practitioner often takes a trial-and-error approach.

²¹In a sense this is just human nature, not specific to machine learning (Baker, 2022).

²²In the context of training machine learning models both big and small, “Goodhart’s law” suggests that this gap is to some extent probably a good thing (<https://openai.com/research/measuring-goodharts-law>).

²³Since the data is random, so is the Fisher information; some authors call this the *observed* Fisher information, in contrast with the *expected* Fisher information (Efron and Hinkley, 1978).

outputs to model probabilities (Denker and LeCun, 1990), and thus at least conceptually, much of the existing statistical methodology can be inherited. For early work in the context of backprop-driven neural networks, MacKay (1992) looks at designing objective criteria for comparing and choosing between models (including norm regularization parameters). MacKay introduces a form of Bayesian “evidence” for candidate models using a Gaussian approximation that requires evaluating the (inverse) Hessian of the base objective function. More generally, the Hessian describes the curvature of the objective function, and is closely related to geometric notions of “flat regions” on the surface induced by the objective function (Goodfellow et al., 2014; Li et al., 2018).

The notion of model complexity has also played a central role in statistical learning theory. It has long been known that even when the number of parameters far outnumber the number of training samples, a small weight norm can be used to guarantee off-sample generalization for empirical risk minimizers (Bartlett, 1998). Of course, due to the high expressive power of neural network models, even with strong weight regularization it is possible to perfectly fit random labels (Zhang et al., 2017), leading to a gap between the test error (chance level) and training error (zero) that is methodologically unsatisfactory. This has motivated a variety of new approaches to measure off-sample generalization (Jiang et al., 2020), as well as to quantify model complexity, such as the degree to which a model can be meaningfully compressed (Arora et al., 2018).

The notion of “flat minima” is seen in the early work of Hochreiter and Schmidhuber (1994, 1997), which considers both how to measure sharpness, and heuristics for actually finding candidates in flat regions. The basic underlying notion is that of measuring “volume,” namely the idea that a “flat” point is one from which we need to go far in most (if not all) directions for the objective function to increase a certain fixed amount. See more recent work by Wu et al. (2017) for related notions of volume in this context. These notions of sharpness are intimately related to properties of the Hessian matrix of the underlying objective function, even when the loss is not based on negative log-likelihood, and an active line of research is centered around the eigenvalue distribution of this Hessian. See for example Chaudhari et al. (2017) and Karakida et al. (2019) for representative work. For sufficiently “regular” models, the determinant of the Fisher information matrix plays a central role in the complexity term used to implement the minimum description length (MDL) principle (Grünwald, 2007); see also early work from Hinton and van Camp (1993) and more recent work by Jia and Su (2020) in the context of neural networks. More generally, however, many neural networks do not satisfy these regularity conditions, and new technical innovations based on the Fisher information have been explored to bridge this gap in recent years (Sun and Nielsen, 2021).

A.3 Algorithms that generalize well

The empirical effectiveness of deep learning goes well beyond what we would expect based purely on learning theoretical insights (Sejnowski, 2020). This success is driven by a handful of workhorse stochastic gradient-based solvers (Schmidt et al., 2021), often coupled with explicit norm-based regularization and a number of techniques used to stabilize learning and effectively constrain the model candidate which is selected by the learning algorithm.²⁴ A rich line of research has developed over the past decade looking at why a certain algorithmic “recipe” tends to generalize well. The tendency for stochastic gradient descent to “escape” from regions near undesirable critical points is one key theme; see Xie et al. (2020) for example.

²⁴These include early stopping, modifying mini-batch size, dropout, batch normalization, stochastic depth, data augmentation, and “mixup” (mixed sample augmentations) among others. See also Montavon et al. (2012) for techniques that were established in the decades before the current wave of deep learning.

For influential work on relating sharpness, mini-batch size, and (weight) norms to off-sample generalization, see [Keskar et al. \(2017\)](#) and [Neyshabur et al. \(2017\)](#). In both papers, the notion of measuring sharpness by a worst-case perturbation appears, and this is pursued even further by [Foret et al. \(2021\)](#) in the well-known sharpness-aware minimization (SAM) algorithm, and extensions due to [Kwon et al. \(2021\)](#) and [Zhao et al. \(2022\)](#). These algorithms, as well as the Fisher information-based procedure of [Jia and Su \(2020\)](#), all involve a forward-difference implementation of explicit gradient regularization (using squared Euclidean norm), and recent work from [Karakida et al. \(2023\)](#) compares this approach with that of direct back-propagation approach. [Barrett and Dherin \(2020\)](#) look at both *implicit* and *explicit* gradient regularization. The implicit side contrasts the path of “continuous” gradient-based updates with the “discrete” updates made in practice (continuous/discrete with respect to *time*), saying that the discrete updates, even when computed based on an unregularized objective function, tend to move closer to the (continuous) path of a regularized objective, where regularization is in terms of the (squared) gradient norms. Inspired by this finding, they also consider explicit GR in the same way; see also [Smith et al. \(2021\)](#).

B Technical appendix

B.1 Additional proofs

Proof of Proposition 1. The machinery of [Cutkosky and Mehta \(2021, Thm. 2\)](#) gives us the ability to control the stationarity of sequences generated using the described procedure (norm-clipping, momentum, normalization), just assuming the “raw” stochastic gradients (here, \mathbf{G}_t) are unbiased estimators of a smooth function. As such, we just need to ensure the assumptions underlying their Theorem 2 (henceforth, [CHT2](#)) are met; the key points have already been described in the main text, so we just fill in the details here. The “unbiased estimator” property we refer to means that we want

$$\mathbf{E}_\mu \mathbf{G}_t(w) = \nabla \tilde{\mathbf{R}}_\mu^{\text{AD}}(w) \quad (19)$$

to hold for all $w \in \mathcal{W}$. Fortunately, this holds under very weak assumptions; the running assumption that $L_{\text{AD}} < \infty$ is more than sufficient.²⁵ In addition, finite L_{AD} also implies that the objective (12) is smooth in the sense that

$$\|\nabla \tilde{\mathbf{R}}_\mu^{\text{AD}}(w_1) - \nabla \tilde{\mathbf{R}}_\mu^{\text{AD}}(w_2)\| \leq L_{\text{AD}} \|w_1 - w_2\| \quad (20)$$

for any $w_1, w_2 \in \mathcal{W}$; this is proved in §B.3. In addition, uniform second moment bounds naturally imply pointwise bounds, so we have

$$\mathbf{E}_\mu \|\nabla \ell(w; \mathbf{Z})\|^2 \leq \mathbf{E}_\mu \left[\sup_{w \in \mathcal{W}} \|\nabla \ell(w; \mathbf{Z})\|^2 \right] \leq L_{\text{AD}} - L_\ell \quad (21)$$

for each $w \in \mathcal{W}$. Taken with the construction of sequence (w_1, w_2, \dots) in the hypothesis, the properties (19)–(21) ensure all the basic requirements of CHT2 are met (with their “ \mathbf{p} ” at 2). Noting that we assume $\mathcal{W} \subseteq \mathbb{R}^d$ using the standard norm and inner product on Euclidean space, the Banach space generality in CHT2 is not needed (their “ C ” and “ p ” can be fixed to 1 and 2 respectively). For reference, the complete upper bound implied by CHT2 is

$$\frac{\tilde{\mathbf{R}}_\mu^{\text{AD}}(w_1) - \tilde{\mathbf{R}}_\mu^{\text{AD}}(w_{T+1})}{T\alpha} + \frac{\alpha L_{\text{AD}}}{2} + \frac{2b\sqrt{L_{\text{AD}} - L_\ell}}{(1-b)T} + \frac{2b\alpha L_{\text{AD}}}{(1-b)} + 2\sqrt{(1-b)(L_{\text{AD}} - L_\ell)}C_\delta \quad (22)$$

²⁵For a more general result, see [Holland \(2023, Lem. 2\)](#) for example.

where for readability the coefficient in the right-most summand is defined by

$$C_\delta := 10 \log(3T/\delta) + 4\sqrt{\log(3T/\delta)} + 1.$$

We have simplified all the terms in CHT2 involving $\max\{1, \log(3T/\delta)\}$, since as long as $T > 0$ and $0 < \delta < 1$, we trivially have $3T/e \geq 1 > \delta$ and thus $\log(3T/\delta) \geq 1$. Furthermore, their free parameters “ b ” (different from our b) and “ s ” are both set to 1, without loss of generality. Plugging in our settings of α and b to the bound in (22) and bounding $(1 - 1/\sqrt{T}) \leq 1$ for readability yields the desired upper bound. \square

Proof of Proposition 2. Here we leverage the projected sub-gradient analysis done by Davis and Drusvyatskiy (2019), in particular their Theorem 3 (henceforth, DDT3). The core of their argument relies upon a weak convexity property held by a rather large class of composite functions, namely compositions of the form $f = h \circ g$, where g is smooth and h is both convex and Lipschitz. Considering the non-smooth objective function

$$w \mapsto \theta + \mathbf{E}_\mu |\ell(w; \mathbf{Z}) - \theta|, \quad (23)$$

it can be taken as a compound function by writing $\mathbf{E}_\mu f(w; \mathbf{Z})$ with $f(w; z) := h(g(w; z))$, where $g(w; z) := \ell(w; z)$ and $h(x) := \theta + |x - \theta|$. Fixing $z \in \mathcal{Z}$ for now, clearly h is 1-Lipschitz and convex. By assumption, we have that $g(\cdot; z)$ is L_ℓ^* -smooth and locally Lipschitz. Then, using standard arguments, it is straightforward to show that $f(\cdot; z)$ is L_ℓ^* -weakly convex.²⁶ Since the weak convexity parameter L_ℓ^* does not depend on the arbitrary choice of z , it follows that the function (23) is L_ℓ^* -weakly convex. In the setting of DDT3, their “ $f(\cdot)$ ” is $\theta + \mathbf{E}_\mu |\ell(w; \cdot; \mathbf{Z}) - \theta|$, and their “ \mathcal{X} ” is \mathcal{W} here. The bound on the expected squared stochastic gradient norms (their “ L^2 ”) is our $L_{\text{AD}} - L_\ell$ just as in the proof of Proposition 1. Finally, the key “unbiased estimator” property in this case deals with sub-differentials, namely we require that

$$\mathbf{E}_\mu \mathbf{G}_t(w) \in \partial \mathbf{E}_\mu |\ell(w; \mathbf{Z}) - \theta| \quad (24)$$

for all $w \in \mathcal{W}$. Fortunately this basic property holds under very weak assumptions that are trivially satisfied when L_{AD} is finite.²⁷ With these facts in place, we simply apply DDT3, in particular their inequality (3.5), with their “ ρ ” corresponding to our L_ℓ^* here, and their “ φ_λ ” corresponding to our (16), with “ λ ” as our β . The desired bound follows by applying their result to the specified procedure over $T - 1$ updates (instead of their T updates). \square

Proof of Proposition 4. To begin, under the assumptions given, the objective (17) clearly inherits the Lipschitz property that the losses have in expectation; since ρ is 1-Lipschitz, we have

$$|\tilde{\mathbf{R}}_\mu(w_1) - \tilde{\mathbf{R}}_\mu(w_2)| \leq \mathbf{E}_\mu |\ell(w_1; \mathbf{Z}) - \ell(w_2; \mathbf{Z})| \leq L \|w_1 - w_2\|. \quad (25)$$

We proceed by using a standard technique for function smoothing.²⁸ If we let \mathbf{V} be a random vector distributed over the unit ball $\{x \in \mathbb{R}^d : \|x\| \leq 1\}$, then regardless of whether $\tilde{\mathbf{R}}_\mu(\cdot)$ is differentiable or not, one can obtain a smooth approximation by averaging over random r -length perturbations, namely

$$\bar{\mathbf{R}}_\mu(w; r) := \mathbf{E} [\tilde{\mathbf{R}}_\mu(w + r\mathbf{V})]. \quad (26)$$

²⁶See for example Drusvyatskiy and Paquette (2019, Lem. 4.2) and Holland (2022, Prop. 8).

²⁷See for example Holland (2022, Prop. 14).

²⁸See for example Flaxman et al. (2004); Nesterov and Spokoiny (2017).

A critical property of the function given in (26) is that it is differentiable and its gradient can be represented explicitly in terms of the function it is trying to smooth, namely we have

$$\nabla \bar{R}_\mu(w; r) = \frac{d}{r} \mathbf{E} [\tilde{R}_\mu(w + r\mathbf{U})\mathbf{U}] = \frac{d}{r} \mathbf{E} [(\theta + \mathbf{E}_\mu \rho(\ell(w + r\mathbf{U}) - \theta)) \mathbf{U}] \quad (27)$$

for any choice of $r > 0$ and $w \in \mathcal{W}$, where \mathbf{U} is uniformly distributed on the unit sphere $\{x \in \mathbb{R}^d : \|x\| = 1\}$ (Flaxman et al., 2004, Lem. 1).²⁹ This means that Lipschitz properties on the original function translate to smoothness properties for the new function. Making this more explicit, using the equality (27), note that for any choice of $w_1, w_2 \in \mathcal{W}$, we have

$$\nabla \bar{R}_\mu(w_1; r) - \nabla \bar{R}_\mu(w_2; r) = \frac{d}{r} \mathbf{E} [(\tilde{R}_\mu(w_1 + r\mathbf{U}) - \tilde{R}_\mu(w_2 + r\mathbf{U})) \mathbf{U}].$$

Taking norms and using the Lipschitz property (25) of \tilde{R}_μ , we observe that

$$\begin{aligned} |\nabla \bar{R}_\mu(w_1; r) - \nabla \bar{R}_\mu(w_2; r)| &\leq \frac{d}{r} \mathbf{E} \|U\| |\tilde{R}_\mu(w_1 + r\mathbf{U}) - \tilde{R}_\mu(w_2 + r\mathbf{U})| \\ &\leq \frac{dL}{r} \|w_1 - w_2\| \end{aligned}$$

and thus have that the smoothed function $\bar{R}_\mu(\cdot; r)$ is (dL/r) -smooth over \mathcal{W} . This means the function is analogous to the objective function (12) used in Proposition 1, except with unbiased stochastic gradients taking the form

$$\mathbf{G}_t(w) := \frac{d}{r} (\theta + \rho(\ell(w + r\mathbf{U}_t; \mathbf{Z}_t) - \theta)) \mathbf{U}_t \quad (28)$$

for $t \geq 1$, where each \mathbf{U}_t is an independent copy of \mathbf{U} from (27). From this point, the remainder of the proof is basically identical to that of Proposition 1; the only remaining changes are the smoothness factor and the second moment bound. For the former, we use dL/r in place of L_{AD} , which also impacts the norm clipping radius γ . For the latter, since we are assuming $w_t + r\mathbf{U}_t \in \mathcal{W}$ for each t , and using the bound (18), we have

$$\mathbf{E} \|\mathbf{G}_t(w)\|^2 \leq \sup_{w \in \mathcal{W}} \left(\frac{d}{r}\right)^2 \mathbf{E} \|\mathbf{U}_t\|^2 (\theta + \rho(\ell(w; \mathbf{Z}_t) - \theta))^2 \leq \left(\frac{d}{r}\right)^2 V.$$

Plugging in these two remaining modified factors to the bounds obtained in Proposition 1 yields the desired result. \square

B.2 Gradient of GR objective

With $w = (w_1, \dots, w_d) \in \mathbb{R}^d$, we will frequently use ∂_j to denote partial derivatives taken with respect to w_j , i.e., for a differentiable function $f : \mathbb{R}^d \rightarrow \mathbb{R}$, we write

$$\partial_j f(w) := \lim_{|a| \rightarrow 0} \frac{f(w_1, \dots, w_j + a, \dots, w_d) - f(w)}{a} \quad (29)$$

with analogous definitions for all $j = 1, \dots, d$. With the above notation in place, note that basic calculus gives us

$$\partial_j \|\nabla R_n(w)\|^2 = \sum_{k=1}^d \partial_j (\partial_k R_n(w))^2 = 2 \sum_{k=1}^d (\partial_k R_n(w)) (\partial_j \partial_k R_n(w)).$$

²⁹Not to be confused with \mathbf{V} in (26), which is uniform on the unit *ball*.

As such, the gradient takes the form

$$\nabla \|\nabla R_n(w)\|^2 = 2\nabla^2 R_n(w) (\nabla R_n(w))$$

where $\nabla^2 R_n$ denotes the $d \times d$ Hessian matrix of R_n , and $\nabla R_n(w)$ is taken as a column vector (a $d \times 1$ matrix) for the purpose of this multiplication.

B.3 Smoothness check

Let us denote the modified gradients concisely as $g(w; z) := \phi(\ell(w; z) - \theta)\nabla\ell(w; z)$. With random variable $Z \sim \mu$, taking any two points $w_1, w_2 \in \mathcal{W}$, based on the equality (10), the normed difference of the gradient expectations can be bounded as

$$\|\mathbf{E}_\mu g(w_1; Z) - \mathbf{E}_\mu g(w_2; Z)\| \leq B_1 + B_2$$

with B_1 and B_2 defined as

$$\begin{aligned} B_1 &:= \mathbf{E}_\mu \|\nabla\ell(w_1; Z)\| |\phi(\ell(w_1; Z) - \theta) - \phi(\ell(w_2; Z) - \theta)| \\ B_2 &:= \mathbf{E}_\mu |\phi(\ell(w_2; Z) - \theta)| \|\nabla\ell(w_1; Z) - \nabla\ell(w_2; Z)\|. \end{aligned}$$

Bounding each of these terms is trivial when the functions ℓ and ϕ are smooth enough. First, note that if ϕ is L_ϕ -Lipschitz and \mathcal{W} is a convex subset of \mathbb{R}^d , we have

$$\begin{aligned} B_1 &\leq L_\phi \mathbf{E}_\mu \|\nabla\ell(w_1; Z)\| |\ell(w_1; Z) - \ell(w_2; Z)| \\ &\leq L_\phi \|w_1 - w_2\| \mathbf{E}_\mu \|\nabla\ell(w_1; Z)\| \sup_{0 < a < 1} \|\nabla\ell(aw_1 + (1-a)w_2; Z)\| \\ &\leq L_\phi \|w_1 - w_2\| \mathbf{E}_\mu \left[\sup_{w \in \mathcal{W}} \|\nabla\ell(w; Z)\|^2 \right], \end{aligned}$$

noting that the second inequality uses the mean value theorem on differentiable $\ell(\cdot; z)$, applied pointwise in $z \in \mathcal{Z}$, and the last inequality uses convexity of \mathcal{W} . This bounds B_1 . Moving on to B_2 , note that if $|\phi(x)|$ is bounded by B_ϕ and the losses are L_ℓ -smooth in expectation, we have

$$\begin{aligned} B_2 &\leq B_\phi \mathbf{E}_\mu \|\nabla\ell(w_1; Z) - \nabla\ell(w_2; Z)\| \\ &\leq B_\phi L_\ell \|w_1 - w_2\|. \end{aligned}$$

Taking these new bounds together, we have

$$\|\mathbf{E}_\mu g(w_1; Z) - \mathbf{E}_\mu g(w_2; Z)\| \leq \left(L_\phi \mathbf{E}_\mu \left[\sup_{w \in \mathcal{W}} \|\nabla\ell(w; Z)\|^2 \right] + B_\phi L_\ell \right) \|w_1 - w_2\|,$$

namely a Lipschitz property in expectation for the modified gradients.

C Empirical appendix

Here we provide additional details and results related to the empirical tests described in §5.

C.1 Linear binary classification

In Figure 9, we compare ERM with Flood and SoftAD run with a *common* threshold level of $\theta = 0.25$, using the (noise-free) “two Gaussians” and “sinusoid” data described in §5.1, and a simple linear model, i.e., a feed-forward neural network with no hidden layers. Training and test sizes match those described in §5.1. Even with a very simple linear model, it is clear that SoftAD can be used to achieve competitive accuracy at much larger loss levels. Note that in the case of “sinusoid,” the average loss does not reach the threshold θ , and thus Flooding is identical to ERM. These basic trends hold over a range of thresholds θ and re-scaling parameters σ (i.e., using $\phi_{\text{al}}((x - \theta)/\sigma)$ with $\sigma \neq 1$). These trends are captured by the heatmaps given in Figure 10, where for each setting of θ (for SoftAD and Flooding) and σ (for SoftAD only), we generate a fresh dataset. Clearly taking the threshold level far too high leads to arbitrarily bad performance, but below a certain level, similar performance is observed over a wide range of values. It is interesting to note how while test loss changes in a rather predictable continuous fashion as a function of θ , the test *accuracy* drops in a much sharper manner when θ is set too high in the case of SoftAD, whereas this drop is smoother in the case of Flooding. That said, these trends are only within the confines of this very simple linear model example using full batch, and tend to change (even with the same model) as we modify the mini-batch size.

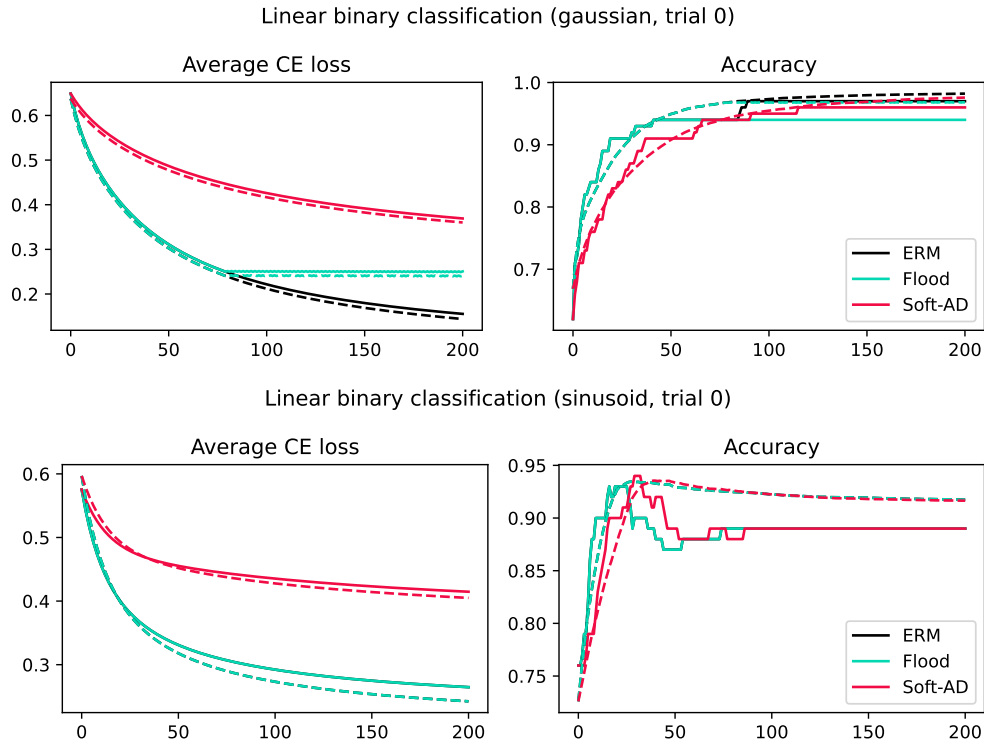


Figure 9: Average cross entropy loss and accuracy over epochs (full batch) for each method.

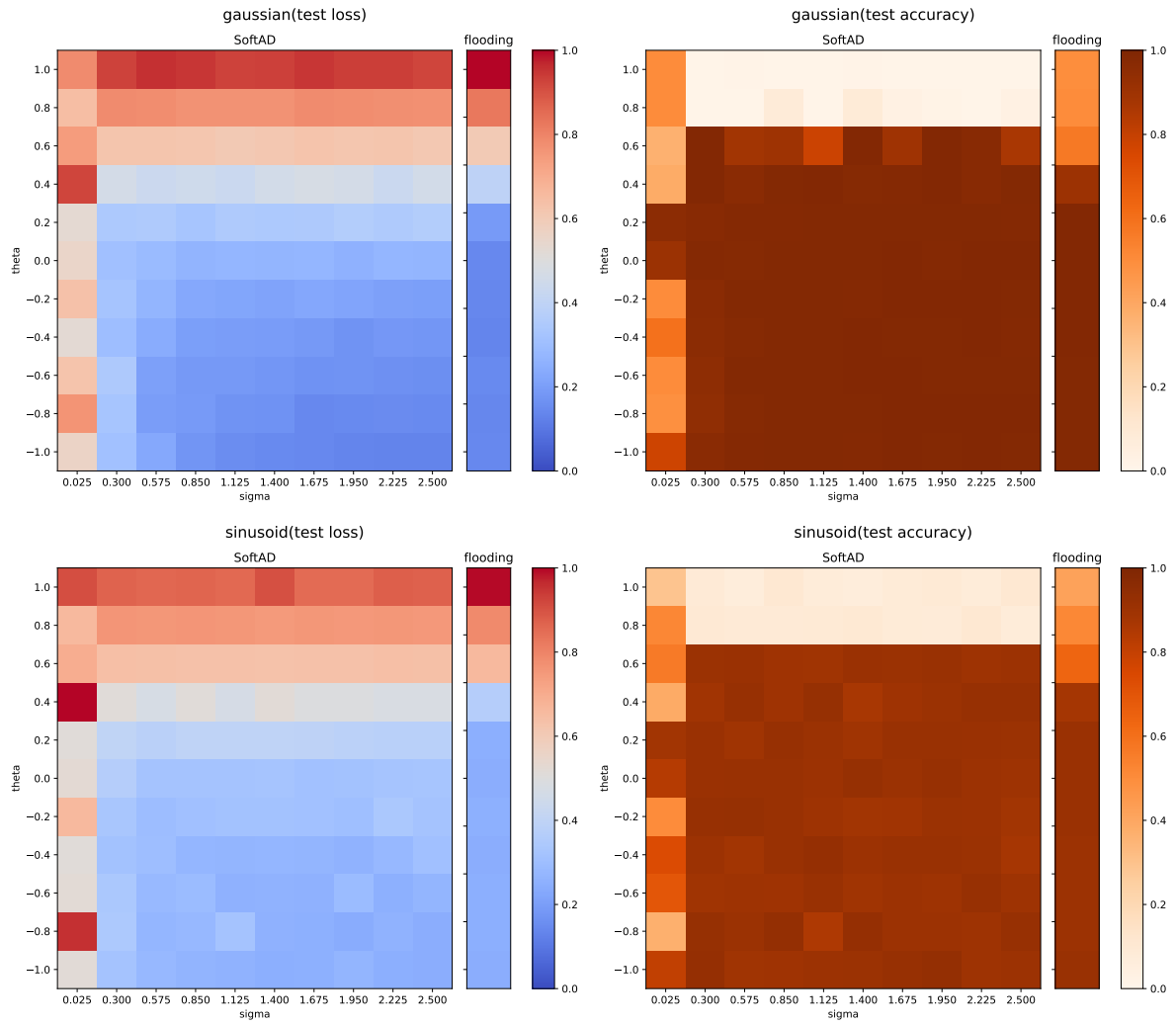


Figure 10: Test loss and accuracy heatmaps for Flooding and SoftAD, depending on threshold level (denoted “ θ ”) and scaling parameter (denoted “ σ ”).

C.2 Supplement to synthetic data tests in §5.1

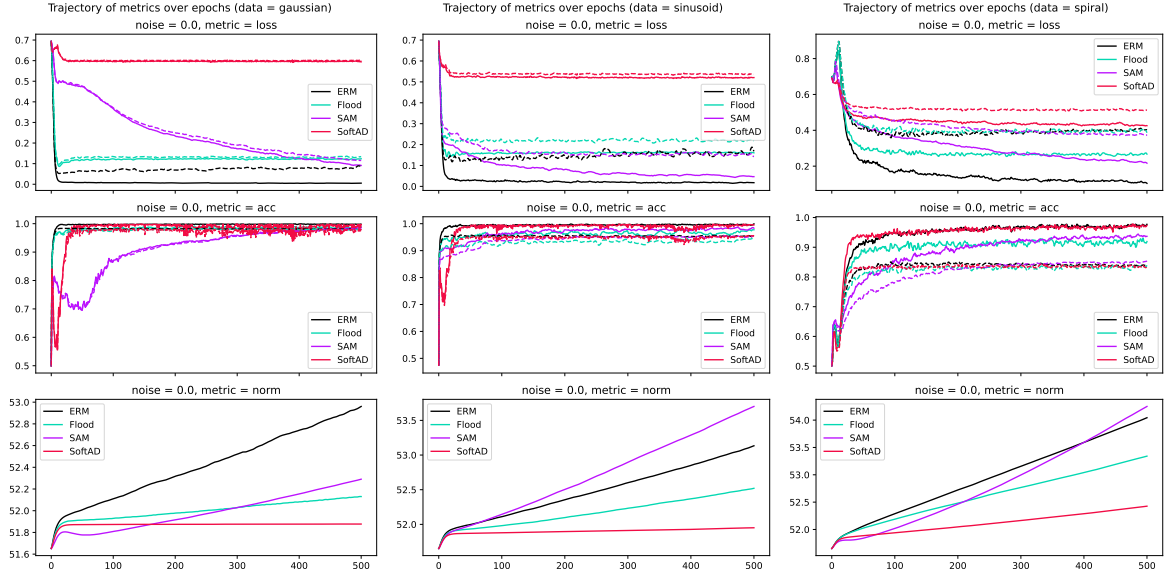


Figure 11: Analogous to Figure 6; all datasets, noise-free, mini-batch of 50.

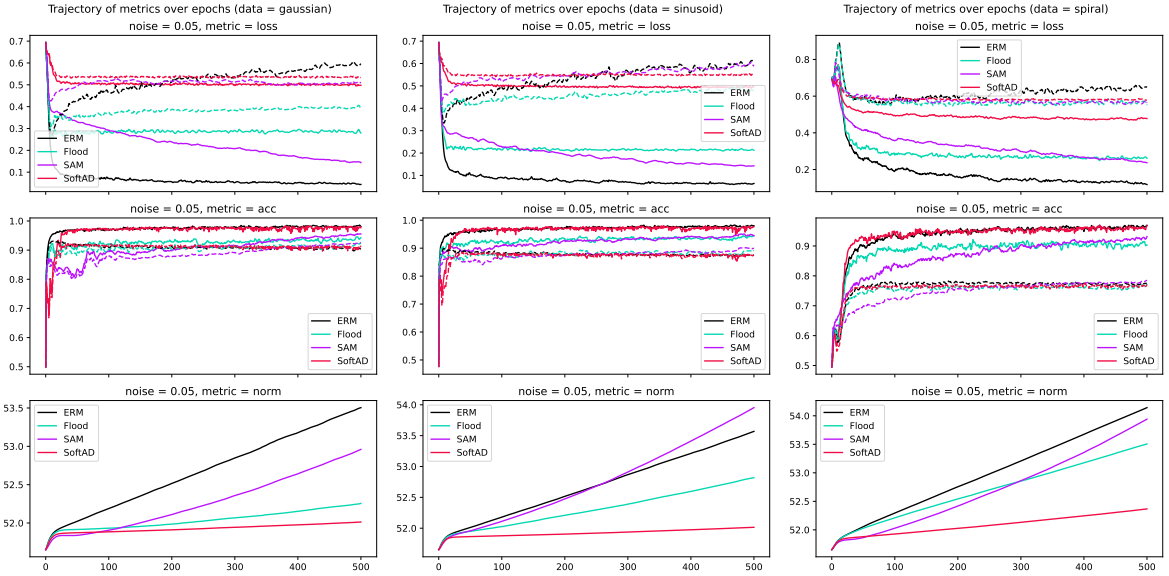


Figure 12: Analogous to Figure 6; all datasets, 5% noisy labels, mini-batch of 50.

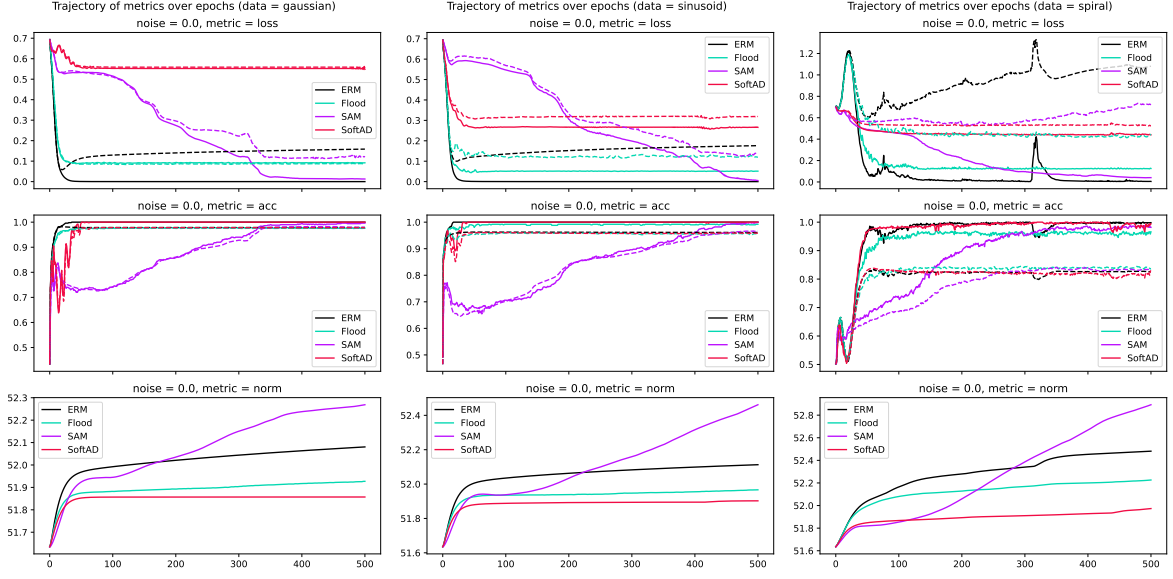


Figure 13: Analogous to Figure 6; all datasets, noise-free, full batch (of 100).

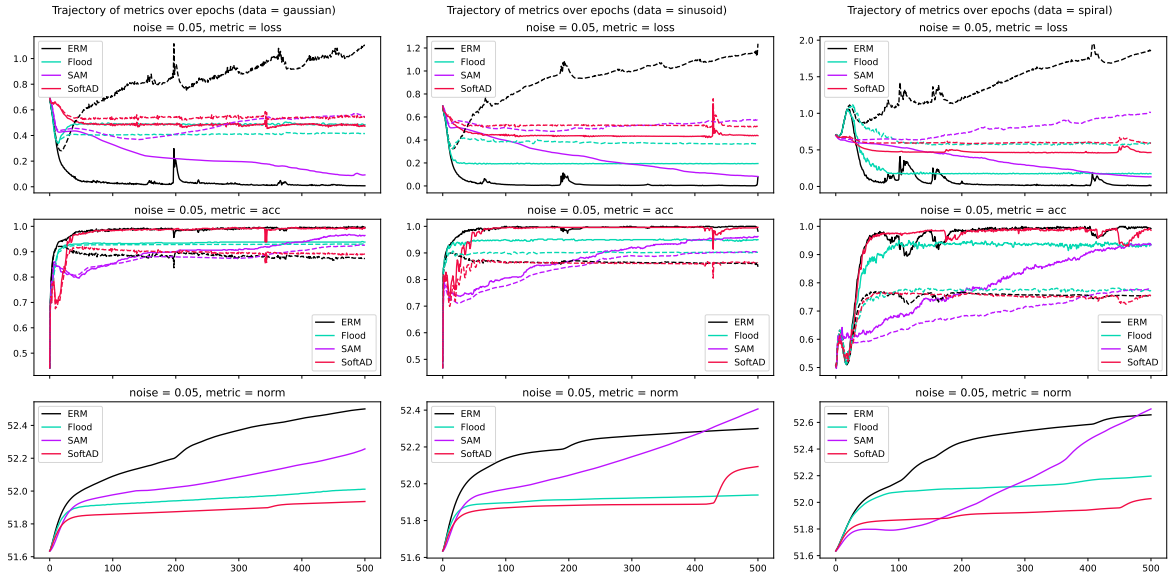


Figure 14: Analogous to Figure 6; all datasets, 5% noisy labels, full batch (of 100).

References

- Arora, S., Ge, R., Neyshabur, B., and Zhang, Y. (2018). Stronger generalization bounds for deep nets via a compression approach. In *Proceedings of the 35th International Conference on Machine Learning (ICML)*, volume 80 of *Proceedings of Machine Learning Research*, pages 254–263.
- Baker, A. (2022). Simplicity. In Zalta, E. N., editor, *The Stanford Encyclopedia of Philosophy*. Metaphysics Research Lab, Stanford University, Summer 2022 edition.
- Barrett, D. G. T. and Dherin, B. (2020). Implicit gradient regularization. *arXiv preprint arXiv:2009.11162*.
- Barron, J. T. (2019). A general and adaptive robust loss function. In *Proceedings of the IEEE/CVF Conference on Computer Vision and Pattern Recognition*, pages 4331–4339.
- Bartlett, P. L. (1998). The sample complexity of pattern classification with neural networks: the size of the weights is more important than the size of the network. *IEEE Transactions on Information Theory*, 44(2):525–536.
- Chaudhari, P., Choromanska, A., Soatto, S., LeCun, Y., Baldassi, C., Borgs, C., Chayes, J., Sagun, L., and Zecchina, R. (2017). Entropy-SGD: Biasing gradient descent into wide valleys. In *International Conference on Learning Representations*.
- Claeskens, G. and Hjort, N. L. (2008). *Model Selection and Model Averaging*. Cambridge Series in Statistical and Probabilistic Mathematics. Cambridge University Press.
- Cutkosky, A. and Mehta, H. (2021). High-probability bounds for non-convex stochastic optimization with heavy tails. In *Advances in Neural Information Processing Systems 34 (NeurIPS 2021)*, pages 4883–4895.
- Cutkosky, A., Mehta, H., and Orabona, F. (2023). Optimal stochastic non-smooth non-convex optimization through online-to-non-convex conversion. *arXiv preprint arXiv:2302.03775v2*.
- Davis, D. and Drusvyatskiy, D. (2019). Stochastic model-based minimization of weakly convex functions. *SIAM Journal on Optimization*, 29(1):207–239.
- Denker, J. and LeCun, Y. (1990). Transforming neural-net output levels to probability distributions. In *Advances in Neural Information Processing Systems 3 (NIPS 1990)*, volume 3.
- Devroye, L., Györfi, L., and Lugosi, G. (1996). *A Probabilistic Theory of Pattern Recognition*, volume 31 of *Stochastic Modelling and Applied Probability*. Springer.
- Dinh, L., Pascanu, R., Bengio, S., and Bengio, Y. (2017). Sharp minima can generalize for deep nets. In *Proceedings of the 34th International Conference on Machine Learning (ICML)*, volume 70 of *Proceedings of Machine Learning Research*, pages 1019–1028.
- Drucker, H. and Le Cun, Y. (1992). Improving generalization performance using double back-propagation. *IEEE Transactions on Neural Networks*, 3(6):991–997.
- Drusvyatskiy, D. and Paquette, C. (2019). Efficiency of minimizing compositions of convex functions and smooth maps. *Mathematical Programming*, 178:503–558.
- Duchi, J. C. and Namkoong, H. (2021). Learning models with uniform performance via distributionally robust optimization. *The Annals of Statistics*, 49(3):1378–1406.

- Dziugaite, G. K., Drouin, A., Neal, B., Rajkumar, N., Caballero, E., Wang, L., Mitliagkas, I., and Roy, D. M. (2020). In search of robust measures of generalization. In *Advances in Neural Information Processing Systems 33 (NeurIPS 2020)*, pages 11723–11733.
- Efron, B. and Hinkley, D. V. (1978). Assessing the accuracy of the maximum likelihood estimator: Observed versus expected Fisher information. *Biometrika*, 65(3):457–483.
- Feldman, V. (2016). Generalization of ERM in stochastic convex optimization: The dimension strikes back. In *Advances in Neural Information Processing Systems 29 (NIPS 2016)*, pages 3576–3584.
- Flaxman, A. D., Kalai, A. T., and McMahan, H. B. (2004). Online convex optimization in the bandit setting: gradient descent without a gradient. *arXiv preprint arXiv:cs/0408007v1*.
- Foret, P., Kleiner, A., Mobahi, H., and Neyshabur, B. (2021). Sharpness-aware minimization for efficiently improving generalization. In *International Conference on Learning Representations*.
- Goodfellow, I. J., Vinyals, O., and Saxe, A. M. (2014). Qualitatively characterizing neural network optimization problems. *arXiv preprint arXiv:1412.6544*.
- Grünwald, P. D. (2007). *The Minimum Description Length Principle*. MIT Press.
- Guo, C., Pleiss, G., Sun, Y., and Weinberger, K. Q. (2017). On calibration of modern neural networks. In *Proceedings of the 34th International Conference on Machine Learning (ICML)*, volume 70 of *Proceedings of Machine Learning Research*, pages 1321–1330.
- Hinton, G. E. and van Camp, D. (1993). Keeping the neural networks simple by minimizing the description length of the weights. In *Proceedings of the 6th Annual Conference on Computational Learning Theory*, pages 5–13.
- Hochreiter, S. and Schmidhuber, J. (1994). Simplifying neural nets by discovering flat minima. In *Advances in Neural Information Processing Systems 7 (NIPS 1994)*.
- Hochreiter, S. and Schmidhuber, J. (1997). Flat minima. *Neural Computation*, 9(1):1–42.
- Holland, M. J. (2022). Learning with risks based on M-location. *Machine Learning*, 111:4679–4718.
- Holland, M. J. (2023). Flexible risk design using bi-directional dispersion. In *Proceedings of the 26th International Conference on Artificial Intelligence and Statistics (AISTATS)*, volume 206 of *Proceedings of Machine Learning Research*, pages 1586–1623.
- Holland, M. J. and Tanabe, K. (2022). Learning criteria going beyond the usual risk. *arXiv preprint arXiv:2110.04996v2*.
- Hu, S., Wang, X., and Lyu, S. (2022). Rank-based decomposable losses in machine learning: A survey. *arXiv preprint arXiv:2207.08768v1*.
- Ishida, T., Yamane, I., Sakai, T., Niu, G., and Sugiyama, M. (2020). Do we need zero training loss after achieving zero training error? In *Proceedings of the 37th International Conference on Machine Learning (ICML)*, volume 119 of *Proceedings of Machine Learning Research*, pages 4604–4614.

- Jia, Z. and Su, H. (2020). Information-theoretic local minima characterization and regularization. In *Proceedings of the 37th International Conference on Machine Learning (ICML)*, volume 119 of *Proceedings of Machine Learning Research*, pages 4773–4783.
- Jiang, Y., Neyshabur, B., Mobahi, H., Krishnan, D., and Bengio, S. (2020). Fantastic generalization measures and where to find them. In *International Conference on Learning Representations*.
- Karakida, R., Akaho, S., and Amari, S.-i. (2019). Universal statistics of Fisher information in deep neural networks: Mean field approach. In *22nd International Conference on Artificial Intelligence and Statistics (AISTATS)*, volume 89 of *Proceedings of Machine Learning Research*, pages 1032–1041.
- Karakida, R., Takase, T., Hayase, T., and Osawa, K. (2023). Understanding gradient regularization in deep learning: Efficient finite-difference computation and implicit bias. In *Proceedings of the 40th International Conference on Machine Learning (ICML)*, volume 202 of *Proceedings of Machine Learning Research*, pages 15809–15827.
- Keskar, N. S., Mudigere, D., Nocedal, J., Smelyanskiy, M., and Tang, P. T. P. (2017). On large-batch training for deep learning: Generalization gap and sharp minima. In *International Conference on Learning Representations*.
- Kullback, S. (1968). *Information Theory and Statistics*. Dover.
- Kwon, J., Kim, J., Park, H., and Choi, I. K. (2021). ASAM: Adaptive sharpness-aware minimization for scale-invariant learning of deep neural networks. In *Proceedings of the 38th International Conference on Machine Learning (ICML)*, volume 139 of *Proceedings of Machine Learning Research*, pages 5905–5914.
- Lee, J., Park, S., and Shin, J. (2020). Learning bounds for risk-sensitive learning. In *Advances in Neural Information Processing Systems 33 (NeurIPS 2020)*, pages 13867–13879.
- Li, H., Xu, Z., Taylor, G., Studer, C., and Goldstein, T. (2018). Visualizing the loss landscape of neural nets. In *Advances in Neural Information Processing Systems 31 (NIPS 2018)*, pages 3576–3584.
- MacKay, D. J. C. (1992). A practical Bayesian framework for backpropagation networks. *Neural Computation*, 4(3):448–472.
- Montavon, G., Orr, G. B., and Müller, K.-R., editors (2012). *Neural Networks: Tricks of the Trade*, volume 7700 of *Lecture Notes in Computer Science*. Springer, 2nd edition.
- Nesterov, Y. and Spokoiny, V. (2017). Random gradient-free minimization of convex functions. *Foundations of Computational Mathematics*, 17(2):527–566.
- Neyshabur, B., Bhojanapalli, S., McAllester, D., and Srebro, N. (2017). Exploring generalization in deep learning. In *Advances in Neural Information Processing Systems 30 (NIPS 2017)*.
- Royset, J. O. (2022). Risk-adaptive approaches to learning and decision making: A survey. *arXiv preprint arXiv:2212.00856*.

- Schmidt, R. M., Schneider, F., and Hennig, P. (2021). Descending through a crowded valley — benchmarking deep learning optimizers. In *Proceedings of the 38th International Conference on Machine Learning (ICML)*, volume 139 of *Proceedings of Machine Learning Research*, pages 9367–9376.
- Sejnowski, T. J. (2020). The unreasonable effectiveness of deep learning in artificial intelligence. *Proceedings of the National Academy of Sciences*, 117(48):30033–30038.
- Shalev-Shwartz, S., Shamir, O., Srebro, N., and Sridharan, K. (2010). Learnability, stability and uniform convergence. *Journal of Machine Learning Research*, 11:2635–2670.
- Smith, S. L., Dherin, B., Barrett, D., and De, S. (2021). On the origin of implicit regularization in stochastic gradient descent. In *International Conference on Learning Representations*.
- Sun, K. and Nielsen, F. (2021). A geometric modeling of Occam’s razor in deep learning. *arXiv preprint arXiv:1905.11027v4*.
- Wu, L., Zhu, Z., and E, W. (2017). Towards understanding generalization of deep learning: Perspective of loss landscapes. *arXiv preprint arXiv:1706.10239*.
- Xie, Z., Sato, I., and Sugiyama, M. (2020). A diffusion theory for deep learning dynamics: Stochastic gradient descent exponentially favors flat minima. *arXiv preprint arXiv:2002.03495*.
- Zhang, C., Bengio, S., Hardt, M., Recht, B., and Vinyals, O. (2017). Understanding deep learning requires rethinking generalization. In *International Conference on Learning Representations*.
- Zhang, J., Karimireddy, S. P., Veit, A., Kim, S., Reddi, S., Kumar, S., and Sra, S. (2020). Why are adaptive methods good for attention models? In *Advances in Neural Information Processing Systems 33 (NeurIPS 2020)*, pages 15383–15393.
- Zhao, Y., Zhang, H., and Hu, X. (2022). Penalizing gradient norm for efficiently improving generalization in deep learning. In *Proceedings of the 39th International Conference on Machine Learning (ICML)*, volume 162 of *Proceedings of Machine Learning Research*, pages 26982–26992.